Appendix A

METRIC

Report on the Production of Monthly Evapotranspiration Maps for the Upper Colorado River Basin for Year 2020 using the METRIC^{tm} Model

submitted to
US Bureau of Reclamation

by
Dr. Richard Allen, Clarence W. Robison and Ayse Kilic
Evapotranspiration, Plus
Twin Falls, Idaho

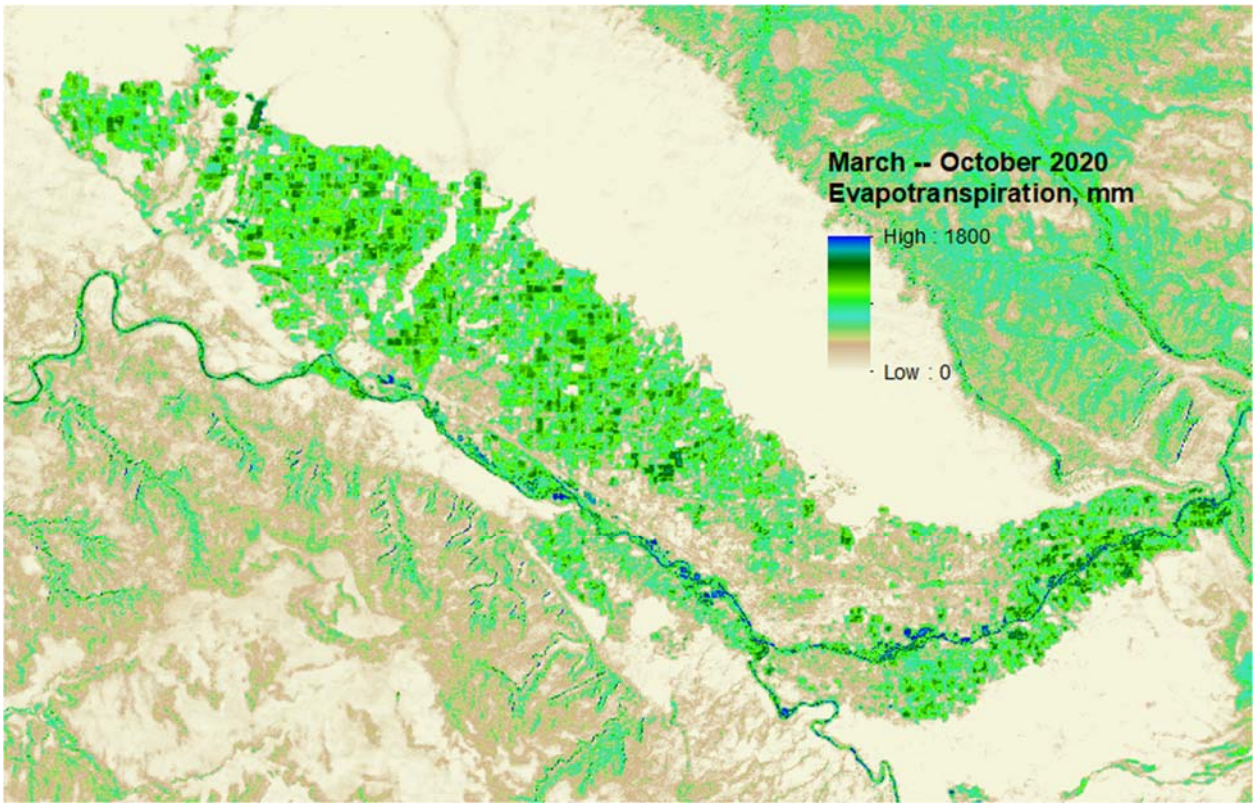

August 2021

Cover Graphic: Extent of ET production for the Fruita Colorado area (Landsat path 36) during 2020, showing higher evapotranspiration as bright green. Beige colored areas have low ET.

Contents

1. Introduction

This report provides a description of the procedures and products used during processing of satellite, weather and land-use data using the METRIC application for the Upper Colorado River Basin for year 2020 to produce spatial maps of monthly evapotranspiration (ET) for the region. Spatial maps of daily ET were produced for specific locations of flux measurement sites. The products represent ET information presented at 30 m resolution in the form of ET (mm per month) and also presented as a fraction of reference evapotranspiration (ET_rF) based on the alfalfa reference crop. The processed region is comprised of four Landsat paths (34, 35, 36 and 37) and three to five Landsat rows per path (30, 31, 32, 33, 34 and 35).

ET was produced using the METRIC model developed by the University of Idaho (Allen et al. 2007a,b; 2011). The METRIC procedure utilizes visible, near-infrared and thermal infrared energy spectrum bands from Landsat satellite images and weather data to calculate ET on a 30 m pixel by pixel basis. ET is estimated from a surface energy balance, where net radiation at the surface (R_n), comprised of both both solar and thermal radiation, is partitioned into ground heat flux (G) and sensible heat flux (H) and ET. The impact of topography of the region on the surface energy balance is incorporated into METRIC via a digital elevation model (DEM), and is used to account for impacts of slope and aspect on solar radiation absorption and impacts of elevation on surface temperature and aerodynamics in complex terrain. The surface energy balance in METRIC was uniquely calibrated for each image date using ground based meteorological information and identified 'anchor' or 'endpoint' conditions (the cold and hot pixels of METRIC) present in each image. A detailed description of METRIC can be found in Allen et al. (2007a,b; 2011).

For the year 2020 processing, a version of the METRIC model that resides on the Google Earth Engine platform named eeMETRIC was used. eeMETRIC is part of the OpenET suite of ET applications and contains all of the METRIC algorithms. eeMETRIC is designed to utilize Earth Engine library functions and collections of Landsat satellite imagery and gridded NLDAS weather data that reside on Earth Engine. Calibration of the surface energy balance in eeMETRIC is completely automated, following Allen et al., (2012) and is done on a scene-by-scene (row-by-row) basis. Estimated accuracy of the automated calibrations averages about +/- 10% relative to an expert, manually-based calibration. Therefore, each scene-date of ET_rF was reviewed, manually, post-eeMETRIC, and a post-adjustment to each ET_rF image was made by stretching the image at both low and high ranges. The adjustment was based on ranges of ET_rF observed in ET_rF vs. NDVI plots and on visual review of the ETrF images. The stretching of the ET_rF image is similar to selecting different calibration end-points in the manually-operated METRIC model due to the near-linear behavior of the model. More detail on review methodology and adjustment is given in Appendix B, including a summary of adjustments for year 2020.

Figure 1 shows the domain of the Landsat images processed by eeMETRIC for year 2020. The figure shows the approximately 160 km x 160 km domains of individual Landsat scenes (path/rows), with overlaps among paths. Also shown, in blue, are major irrigated regions and important automated weather stations as black points.

2. Image Selection and pre-processing

Imagery from Landsat satellites is utilized in eeMETRIC to take advantage of the relatively high resolution of 30 m and the presence of a thermal band. The 30 m resolution provides ET information at the sub-field scale, which is important for agricultural water management and for water rights

management. The thermal information permits application of a surface energy balance that is able to determine ET under both well-watered and stressed conditions. For 2020, images from both Landsat 8 and Landsat 7 satellites were processed. Landsat 7 was launched in 1999. Landsat 8 was launched in February 2013.

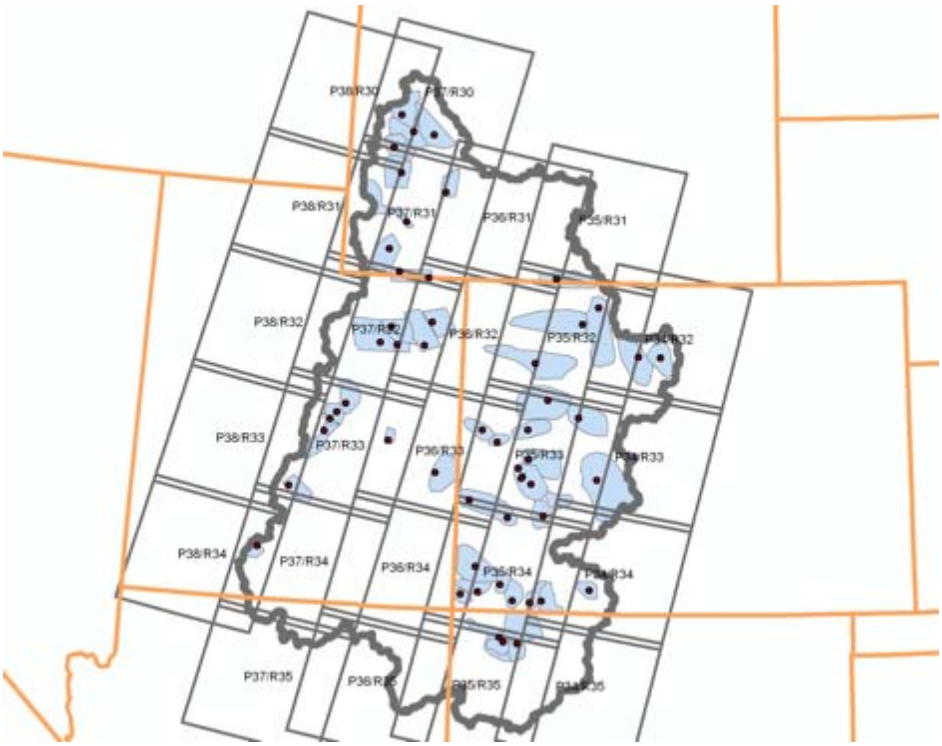

Figure 1. Overlays of Landsat scenes onto the Upper Colorado River Basin (thick grey line), with path 34 on the east and path 37 (and 38) on the west. Major irrigated areas are shown in blue with primary automated weather stations as black dots. State outlines are shown in orange.

Landsat 7 images acquired after May 2003 are less preferred than from Landsats 8. This is due to an anomaly with the Landsat 7 satellite caused by the malfunction of the scan line corrector (SLC-off) beginning in May 2003. As a consequence, Landsat 7 images processed for year 2020 are "SLC-off" images that contain wedge shaped gaps extending from the edges of the image and stretching towards the centers, as shown later in Figure 4.

An important criterion for image selection is an assessment of cloud conditions at the time of the satellite overpass. The clearness of the atmosphere is impacted by clouds, including thin cirrus clouds, and jet contrails, smoke and haze. The occurrence of these conditions over an area of interest can render that part of the image unusable for processing in METRIC. Even very thin cirrus clouds can produce lower surface temperature than the actual ground surface. Because METRIC uses surface temperature estimates to solve the energy balance, areas having cloud cover create error in the ET estimates. In addition, areas recently shaded by moving clouds may appear to be cooler than other sunlit areas because they have not yet reached a thermal equilibrium corresponding to the clear sky energy loading. Areas adjacent to clouds and shadows are generally masked out of the processed images and replaced with information from other image dates, as described later.

Initial cloud assessment was done during scene (date) selection by viewing Landsat preview images at http://glovis.usgs.gov/ and noting the amount of cloud cover in the image, especially over irrigated regions in the scene. Special preference was given for clearness over irrigated areas of the study area. The scene lists selected during initial cloud scoring were used to direct the processing by the eeMETRIC model on Google Earth Engine. Following processing, Landsat images processed into ET_rF were downloaded from Earth Engine in UTM projection and coordinate system. The UTM projection was converted into an Albers Equal Area projection that was designed by USBR to describe geometric information over the entire UCRB. The customized Albers Equal Area has the attributes: latitude of origin: 34°; central meridian: -109 °; 1st standard parallel: 36.8333333333 °; 2nd standard parallel: 42.1666666667 °; false easting: 500000 m; false northing: 0 datum: NAD83, output format: geotiff, output pixel size: 30 m, and resampling method of cubic convolution (CC).

A total of 523 Landsat images were processed for paths 34-37 using eeMETRIC on the Google Earth Engine and were downloaded as geotif files. The selection of image dates was according to clearness of the images over irrigated areas and the dates of the images relative to other images. The ET_rF images were manually reviewed and adjusted by stretching ETrF images at high and/or low ends of the ET_rF spectrum based on review of plots of ET_rF vs. NDVI and by visual inspection of ET_rF and NDVI images. The objective of the adjustments was to produce ET_rF images that had an upper distribution of ET_rF around values of 1.0 and a lower distribution of ET_rF lying close to the estimated ET_rF resulting from residual evaporation from recent precipitation. Adjustments to images averaged about 0.0 to 0.1 ET_rF, with an occasional adjustment of 0.3 or more for late winter images or for substantially clouded or substantially wet image dates where the automated calibration failed to produce a dependable ET_rF image.

The 523 image dates were filtered to 418 image dates to remove image dates that were judged to be too cloudy to be dependably used during time integration, or were not needed for time integration due to their dates being well before or well after the March-October growing period or the presence of other dependable ETrF image dates close in time. This was sometimes the case when a viable Landsat 7 image lay eight days from a viable Landsat 8 image. In that situation, the Landsat 7 image, because of its SLC-off deficiencies, was removed from integration to provide the adjacent Landsat 8 image with more impact on the time integration process for producing monthly products. In other cases, an individual scene-date was removed if other scenes in the same path on a particular date were missing due to cloudiness. In general, one or more images were processed for each month, up to four. This tended to insure that there was ET information generated for each of the 30 million pixels of an image for a cloud-free condition. Each Landsat path has unique dates that are different from adjacent paths and must be processed separately in METRIC due to varying weather conditions and surface temperatures. A full list of Landsat scene dates is included in Appendix A. In total, about 15 billion pixel/dates were processed for ET_rF for year 2020, with 12 billion pixel/dates used during time integration. The four path coverage of the UCRB encompassed approximately 500 million 30-m Landsat pixels. Table 1 of Appendix A provides a summary of the scene-dates by path and row processed by eeMETRIC and the numbers used during time integration of ET to monthly values. In the end, 201 Landsat 8 scenes were processed by eeMETRIC and used during time integration and 52 Landsat 8 scenes were processed, but not used during time integration for reasons described previously. There were 216 Landsat 7 scenes processed and used during time integration and 51 Landsat 7 scenes processed but not used during time integration.

General features of the basin

The Upper Colorado River basin has a semi-arid climate with low amounts of precipitation at low elevations and increasing precipitation over higher elevation mountainous. Vegetation types and densities are generally associated with precipitation levels. Irrigated agriculture is generally distributed in groups of development near major river systems, or along small streams, especially in mountain valleys.

A mosaic of Landsat scenes within the Upper Colorado River Basin (thick grey line) is displayed in figure 2 showing a "false color" three band image where vegetation is displayed as green and low vegetation areas show as light to dark purple. Irrigated areas are difficult to see, due to their relatively small size, but tend to show as a lighter green color. Forested mountain areas dominate the eastern part of the basin.

DEM and Land Use maps used for METRIC processing

Other basic input files utilized during eeMETRIC processing, besides the satellite images, include a Digital Elevation Model (DEM) and Land Use (LU) images. The DEM is used during eeMETRIC processing to adjust surface temperatures for lapse effects caused by elevation variation. In addition, maps of slope and aspect (aspect is the cardinal direction of an inclined surface) are derived from the DEM at 30 m resolution and are used to estimate solar radiation on slopes and in defining aerodynamics of heat convection in mountains.

Because eeMETRIC runs within the Google Earth Engine Platform, it needs to use data collections housed inside Earth Engine. This includes the DEM product, which, for eeMETRIC is the Shuttle Radar Topography Mission (SRTM) version 3.0 product having 30 m spatial resolution. This constrasts with the 2017 use of the USBR produced and distributed a 30-meter DEM in the customized Albers projection described earlier. That DEM was generated from the latest USGS 1 arc-second NED data that were downloaded in 2017 from the USGS, and resampled to a 30-meter grid using bilinear interpolation. A visual overview of elevation features in the UCRB is shown in Figure 3, where high elevations are shown as lighter shades of grey.

A land use (LU) map was used to support the estimation of aerodynamic roughness and soil heat flux during eeMETRIC processing. For year 2020, the 2016 NLCD (National Land Cover Database, 2011) Land Use map housed in Earth Engine was accessed by eeMETRIC.

3. The eeMETRIC Model

METRIC™ (Mapping Evapotranspiration with high Resolution and Internalized Calibration) bases the ET estimate on the evaluation of the energy balance at the earth's surface. METRIC™ processes instantaneous remotely-sensed digital and weather data and estimates the partitioning of energy into net incoming radiation (R_n), heat flux into the ground (G), sensible heat flux to the air (H), and latent heat flux (LE). The latent heat flux is computed as a residual in the energy balance, represents the energy consumed by ET:

$$LE = R_n - G - H \quad (1)$$

where LE = latent energy consumed by ET; R_n = net radiation; G = sensible heat flux conducted into the ground; and H = sensible heat flux convected to the air. Determining LE by energy balance keys off the large energy required to transform liquid water to vapor. The main advantage of using an energy balance is that actual ET is computed, rather than a potential ET that is based on amount of vegetation, so that any reductions in ET caused by shortage of soil moisture are captured in the ET estimate. In traditional applications of energy balance, the computation of LE is only as accurate as the summed estimates for R_n, G, and H. For this reason, eeMETRIC employs a calibration strategy to overcome systematic biases in R_n and G by focusing the internal calibration on LE, with H used to assimilate intermediate estimation errors and biases.

METRIC™ utilizes spectral raster images from the visible, near infrared, and thermal infrared energy spectrum to compute the energy balance on a pixel-by-pixel basis. In METRIC, R_n is computed from the satellite-measured narrow-band reflectance and radiometric surface temperature; G is estimated from R_n, radiometric surface temperature, sensible heat flux and vegetation indices; and H is estimated from surface temperature ranges, surface roughness, and wind speed using buoyancy corrections. Figure 4 shows a general schematic of the METRIC process.

eeMETRIC is calibrated uniquely, but in a fully automated manner, for each image date and scene because of the unique surface temperature conditions occurring on each image date and changing weather conditions including wind speed and air humidity. The main objective of calibration is the production of accurate estimates of ET from lands having agricultural production. This is done because of the high importance of ET from agricultural areas. Calibration settings focus on agricultural areas because of their more uniform and predictable behavior which improves the accuracy of the calibration of the sensible heat flux function of METRIC. The calibration of METRIC automatically transfers to other land use types in an image, including forest and rangeland. eeMETRIC employs a completely automated calibration technique that is based on statistical distributions of NDVI and surface temperature following Allen et al. (2012) and complemented by a special planar delapsing scheme developed for eeMETRIC by ReVelle, Kilic and Allen during the OpenET development. That scheme is described on the OpenET 2021 web site.

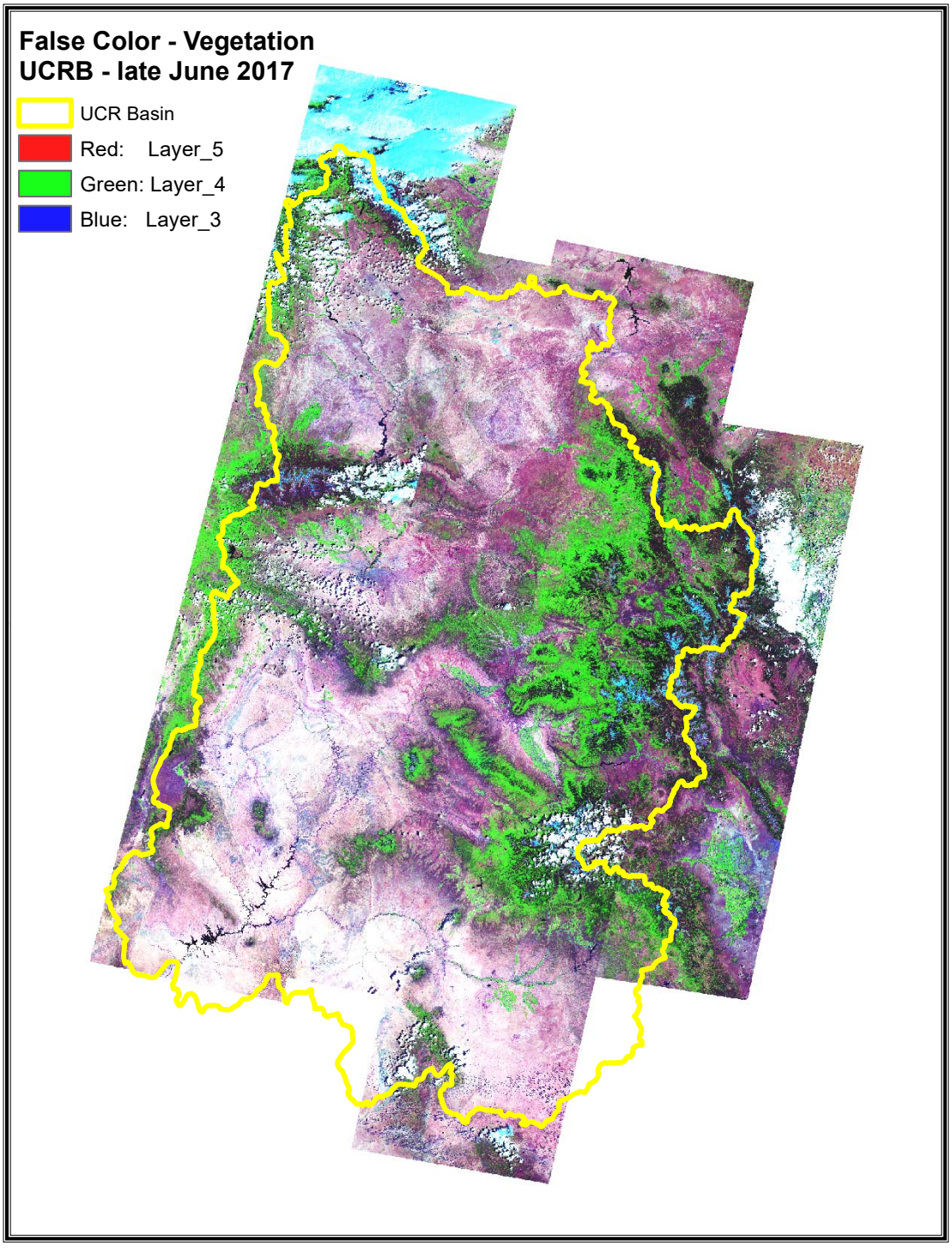

Figure 2. A mosaic of Landsat scenes within the Upper Colorado River Basin (thick yellow line) showing a "false color" three band image result where vegetation is displayed as green and low vegetation areas show as light to dark purple. Irrigated areas are difficult to see, due to the small scale, but tend to show as a lighter green color. Forested mountain areas dominate the eastern part of the basin.

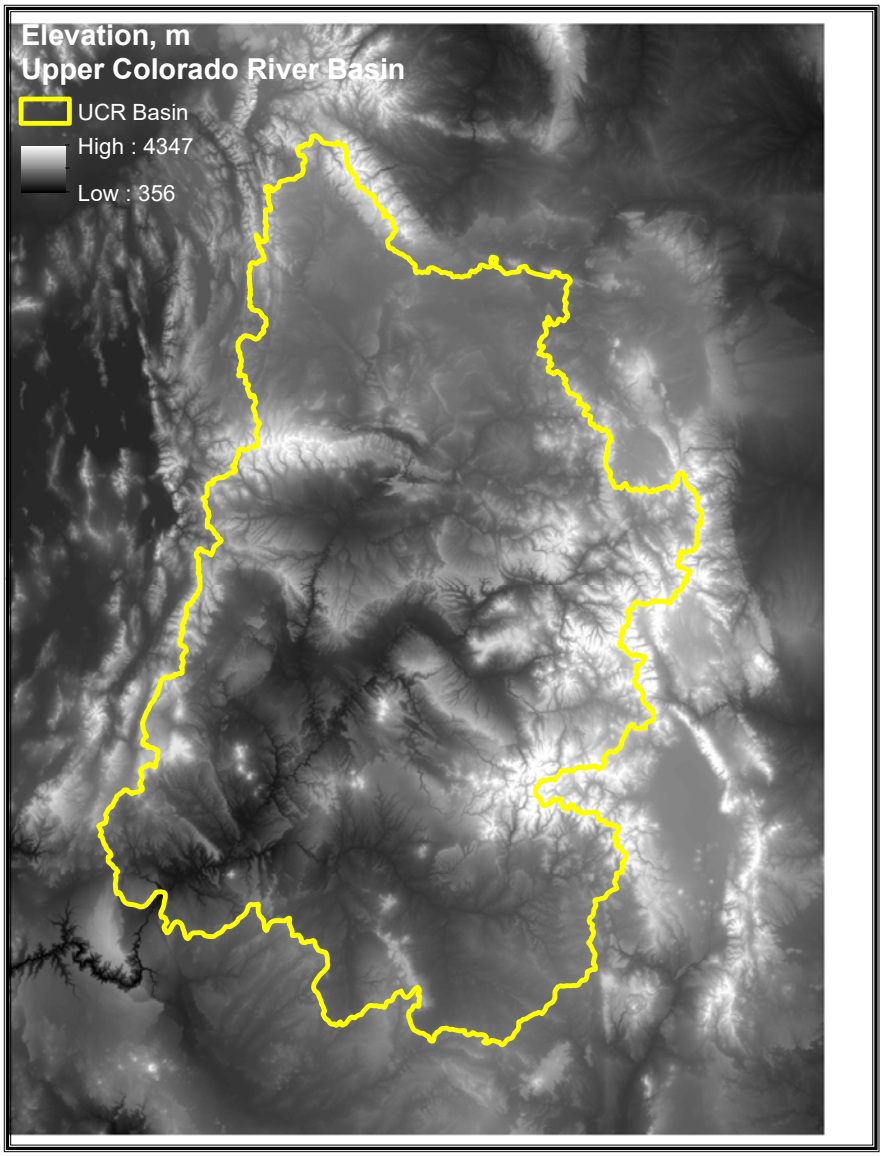

Figure 3. Elevations of the Upper Colorado River Basin where higher elevations show as lighter shades of grey.

Evaporation from open water is estimated in eeMETRIC using an aerodynamic evaporation algorithm rather than using the energy balance for increased accuracy. In the energy balance for open water, parameter G (heat storage flux into water) is large and uncertain. Therefore, evaporation is estimated using a standard aerodynamic estimation equation (Jensen and Allen, 2016) using a saturation specific humidity at the water surface that is based on the surface temperature image and using an estimate of specific humidity of the air above the water surface based on the assumption of constant relative humidity across the image. That assumption is supported by behavior of relative humidity in gridded weather data sets. The aerodynamic resistance term in the aerodynamic equation is estimated by extrapolating wind speed at a 200 m blending height (determined by extrapolating wind speed from a weather station to 200 m) down to the water surface using an aerodynamic roughness estimate for open water. Details are given in Allen et al. (2014).

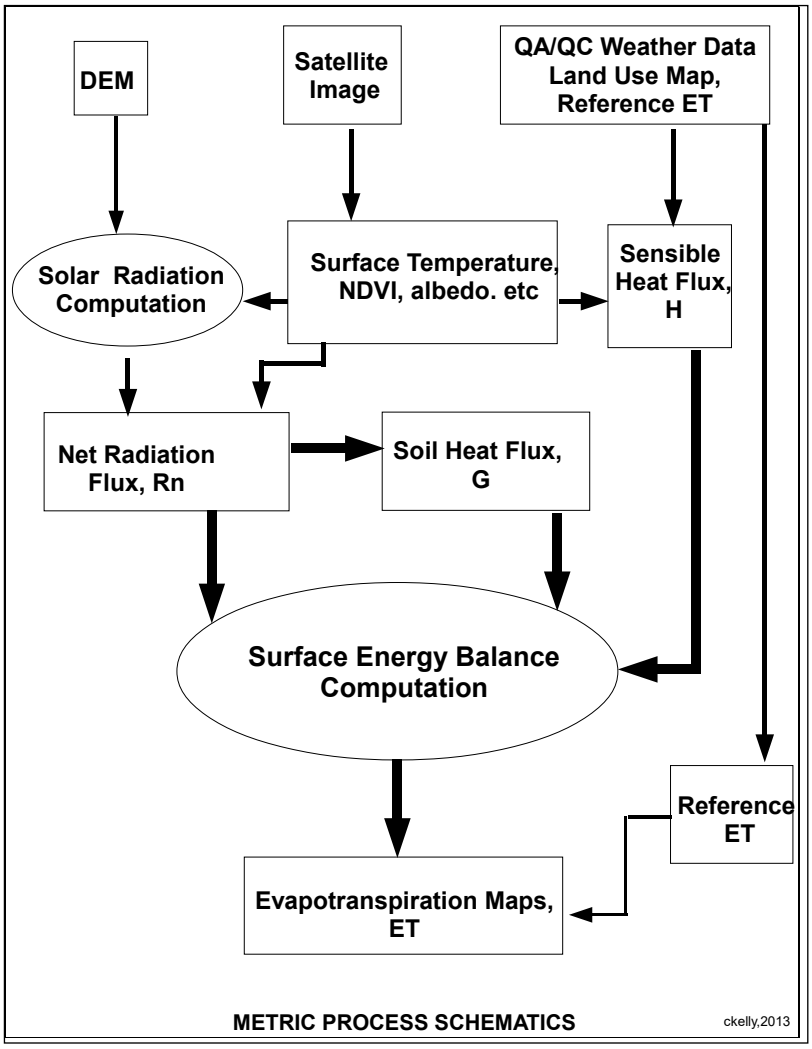

Figure 4. General schematic of the eeMETRIC processes.

The eeMETRIC code used in the UCRB application is a Python-coded model that utilizes Google Earth Engine image processing functions. The model was run via an Earth Engine application programming interface (API) on Earth Engine for a sequence of scenes and image dates, with processed images downloaded from a Google Drive as geotiff ETrF and NDVI files. The geotiff files were reprojected to the special Upper Colorado River Basin Albers Conical Equal Area projection after downloading from Earth Engine and prior to mosiacing rows within paths for common overpass dates.

4. Weather data processing

eeMETRIC utilizes alfalfa reference ET (i.e., ET_r) as calculated by the ASCE standardized Penman-Monteith equation (ASCE-EWRI 2005; Jensen and Allen 2016) for calibration of the energy balance process and to establish a daily soil water balance to estimate residual soil evaporation from bare soil following precipitation events (Allen et al. 2007a). Hourly ET_r is used as a means to 'anchor' the surface energy balance by representing the ET from locations having high levels of vegetation and cooler radiometric surface temperatures. In eeMETRIC, hourly data are derived from the North American Land Data Assimilation System (NLDAS) (https://ldas.gsfc.nasa.gov/nldas/) (Cosgrove et al., 2003). Those data are used for calibration of the surface energy balance. Twenty-four hour weather data are obtained from the GridMet gridded weather data (Abatzoglou John T., 2013) on Earth Engine and are used to

calculate daily reference ET that is used with precipitation from GridMet to evaluate background evaporation at satellite overpass time using a daily soil evaporation model. Grid size is approximately 12 km for NLDAS data and 4 km for daily GridMet data.

The soil water balance is based on the two-stage daily soil evaporation model of the United Nations Food and Agriculture Organization's Irrigation and Drainage Paper 56 (Allen et al 1998). The procedure employs the skin evaporation enhancement of Allen (2011) that increases the magnitude of evaporation spikes following light precipitation events.

Hourly data from agricultural weather stations in each path were used to conduct daily soil water balances to estimate background evaporation at overpass time. These estimates were used to assess expected ET_rF for low vegetation conditions during review of ET_rF images. One to two weather stations were selected for each path. The stations evaluated and selected are operated by the Pacific Northwest Cooperative Agricultural Network (AGRIMET) of the US Bureau of Reclamation and by the Colorado Agricultural Meteorological system (CoAgMet). The coordinates and characteristics of the meteorological stations, and general comments, are summarized in Table 1.

Table 1. Characteristics of the weather stations used for calculating daily soil water balances and evaporation estimation that were consulted during during review and adjustment of eeMETRIC images for year 2020.

Landsat Path	Station	Network	Comments
37	Boulder, Wyo	Agrimet and HPRCC	
36, 37	Pelican Lake, UT	Agrimet	On the dry side during summer, RH ranging from 10 to 70%
35	Delta, CO	Coagmet/Agrimet	
34	Gunnison (w/35)	Coagmet/Agrimet	Low wind speed at night (< 1 m/s). Good Rs, good RH environment. 7900 ft. elev.

Daily ET_r used for time integration. For time integration of ET over periods between Landsat image dates, a complete, daily surface of alfalfa ET_r was constructed by the Desert Research Institute and provided to USBR for resampling to 510 m prior to use in this study. Details on that surface, including the data sources (GridMET) and bias correction to data, are presented in the DRI report.

5. METRIC™ processing and results

eeMETRIC produces 30x30 m spatial resolution maps of both ET_rF (Fraction of Alfalfa Reference Evapotranspiration) and actual ET. The main products produced are:

- Daily ET_rF and ET maps for every image date.

- Monthly ET, ET_rF and ET_r maps.
- Summary (multi month) ET, ET_rF and ET_r maps.

Treatment of SLC-Off Gaps for Landsat 7 images

Landsat 7 images acquired after May 2003 have information gaps caused by the malfunction of the scan line corrector (SLC). As a result, Landsat 7 images were "SLC-off" images where wedge shaped gaps exist in the images, extending from the edges of the image and stretching towards the centers, as shown in Figure 6. Full description of the SLC-off malfunction is provided at USGS web sites (http://landsat.usgs.gov/products_slcoffbackground.php). The SLC-off gaps were treated as clouds for year 2020 to be more consistent with a similar practice used with the OpenET ET models that were applied independently for the UCRB for year 2020. The consistency allowed for a focused comparison of impacts of the manual review and adjustment procedure used in this study with eeMETRIC and the fully automated applications of OpenET where no adjustments are possible.

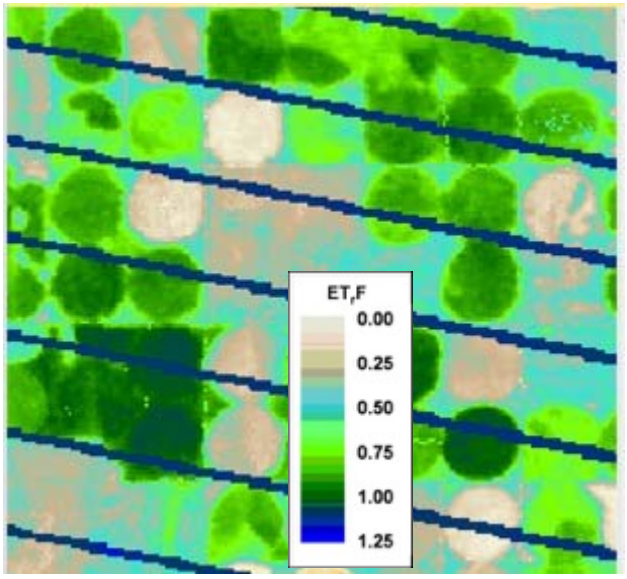

Figure 6. Close-up of a Landsat-based ET_rF image showing gaps (stripes) in ET_rF originating from the SLC-off gaps in a Landsat 7 image..

Dealing with clouded parts of images

Satellite images often have clouds in portions of the images, and paths 34-37 in the UCRB are no exception. ET_rF cannot be directly estimated for clouded areas using surface energy balance because cloud temperature masks surface temperature and cloud albedo masks surface albedo. In manual applications of METRIC, it is generally preferred to fill in ET_rF for clouded areas prior to time integration for producing monthly ET. Cloud mask filling provides for better, manual control of the 'donor' ET_rF material that comes from adjacent image dates where the user can adjust for differences in background evaporation from wetting events that stem from the different image dates (Kjaersgaard et al., 2011). The background evaporation adjustment to cloud-filled areas was not applied here, however, due to time and budget limitations and the desire to automate most processes to the extent possible. In some high elevation areas, clouded (or 'missing') portions of an image sometimes resulted in long periods between valid ET_rF data (sometimes longer than several months).

Clouds and shadows were identified for year 2020 using the BQA product produced by the USGS EROS center for each Landsat image. The resulting cloud/shadow mask (1 -cloud or shadow, 0 -clear)

was despeckled using a focal minimum function on a 3x3 pixel kernel. That function removed clusters of masked pixels having sizes of three pixels or less. Those speckles were, in many cases, caused by misidentification of large buildings or small ponds as clouds. The despeckled cloud/shadow mask was then dilated using a 15 x 15 pixel focal maximum function followed by a 15 x 15 pixel focal majority function. The focal maximum function expanded and smoothed edges of masked regions and the focal majority further smoothed and merged masked regions. The net effect was expansion of cloud and shadow masked areas from the BQA product by about 500 m.

The buffering worked relatively well in expanding the original cloud/shadow mask and to reduce the occurrence of small clear pixel inclusions within larger clouded areas. The buffering expanded cloud/shadow masks outward to cover areas adjacent to the originally marked clouds and shadows. The benefit of the expansion of the masks are that the expansion areas often exhibited cool thermal artifacts stemming from recent cloud movement, or due to the BQA product missing impacted areas near cloud edges. Masking these areas was intended to reduce error in the ET estimates caused by a false cool thermal signal. Buffered areas tended to mask areas near clouds that were in direct sunlight at the time of the satellite overpass, but may have been shaded a few minutes earlier, due to cloud movement, and therefore may have been colder than temperatures associated with the surface energy balance, and therefore would give inaccurate estimates of ET. Observation of ET_rF near BQA masked areas indicated that some thermal effects of clouds and shadows were present up to 2000 m from the BQA masks, which were relatively conservative. Therefore, the expansion of BQA masks by 500 m was a conservative procedure that may still have left some cloud/shadow artifacts in adjacent areas. Figure 7 shows an example of a close up of a BQA cloud/shadow mask and the same result following buffering.

ET_rF of cloud/shadow masked areas associated with an image were not used in the linear interpolation of daily ET_rF but were instead replaced by ET_rF values interpolated from before and after images when the area was cloud free. For example if an area was cloudy on April 12, the ET_rF for the area was based on linear interpolation between March 19th and April 20th provided the area was cloud free for those image dates.

Mountainous areas tended to have more incidences of cloud cover for Landsat images, as expected, due to orographic cooling effects and uplift of air masses. During the time integration of Landsat ET_rF images into monthly and growing season totals, pixel by pixel counts of numbers of clear scene dates vs. numbers of clouded scene dates were recorded. Figure 8 shows a map of percent clear scenes for every pixel across the basin. Availability of clear pixels was lowest at high elevations, and somewhat greater in the southern portion of the basin, as expected. As indicated in Table 1 of Appendix A, an average of about 29 scene dates were processed for each path/row and used during time integration to obtain monthly ET. Numbers of dates ranged from 27 for path 37 to 30 for path 35. Frequent occurences of clouds accentuated the impacts of L7 SLC-off gaps, as missing data in gaps lengthed time periods between valid data. The BQA from EROS band tended to mis-identify stream/lake/reservoir edges as clouds, especially during cooler periods. As a result, most of the streams and water bodies showed as clouds and were therefore incorrectly buffered out in a number of images, as shown in Figure 8. This created uncertainty in open water evaporation estimates by METRIC that are based on the aerodynamic method. This was unable to be rectified.

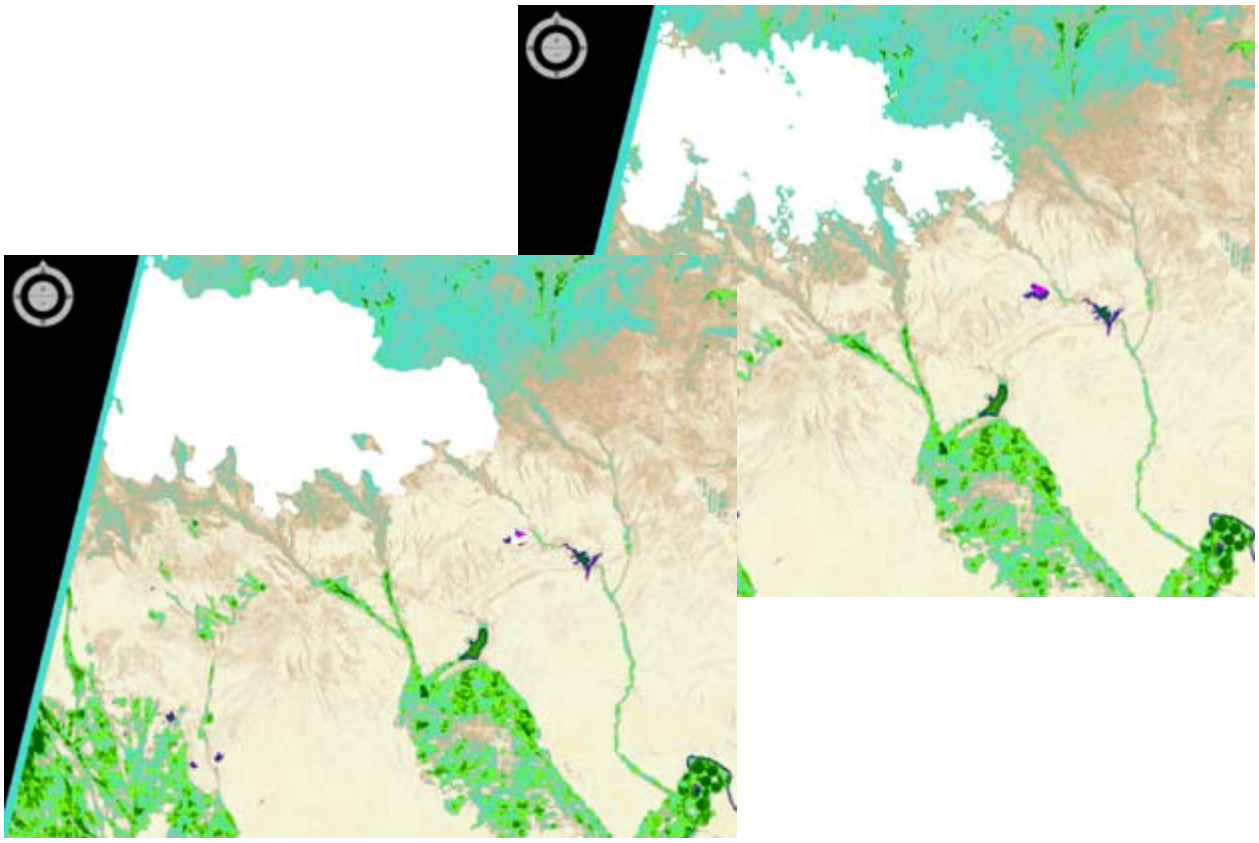

Figure 7. Left: Close-up of an ET_rF image for 6/22/2017 (P36) near the Pelican Lake, UT area, showing cloud masked areas (white areas) overlying a colorized ET image. The top figure shows the original cloud/shadow masked area from the EROS BQA product in white. The bottom image shows the same area following buffering.

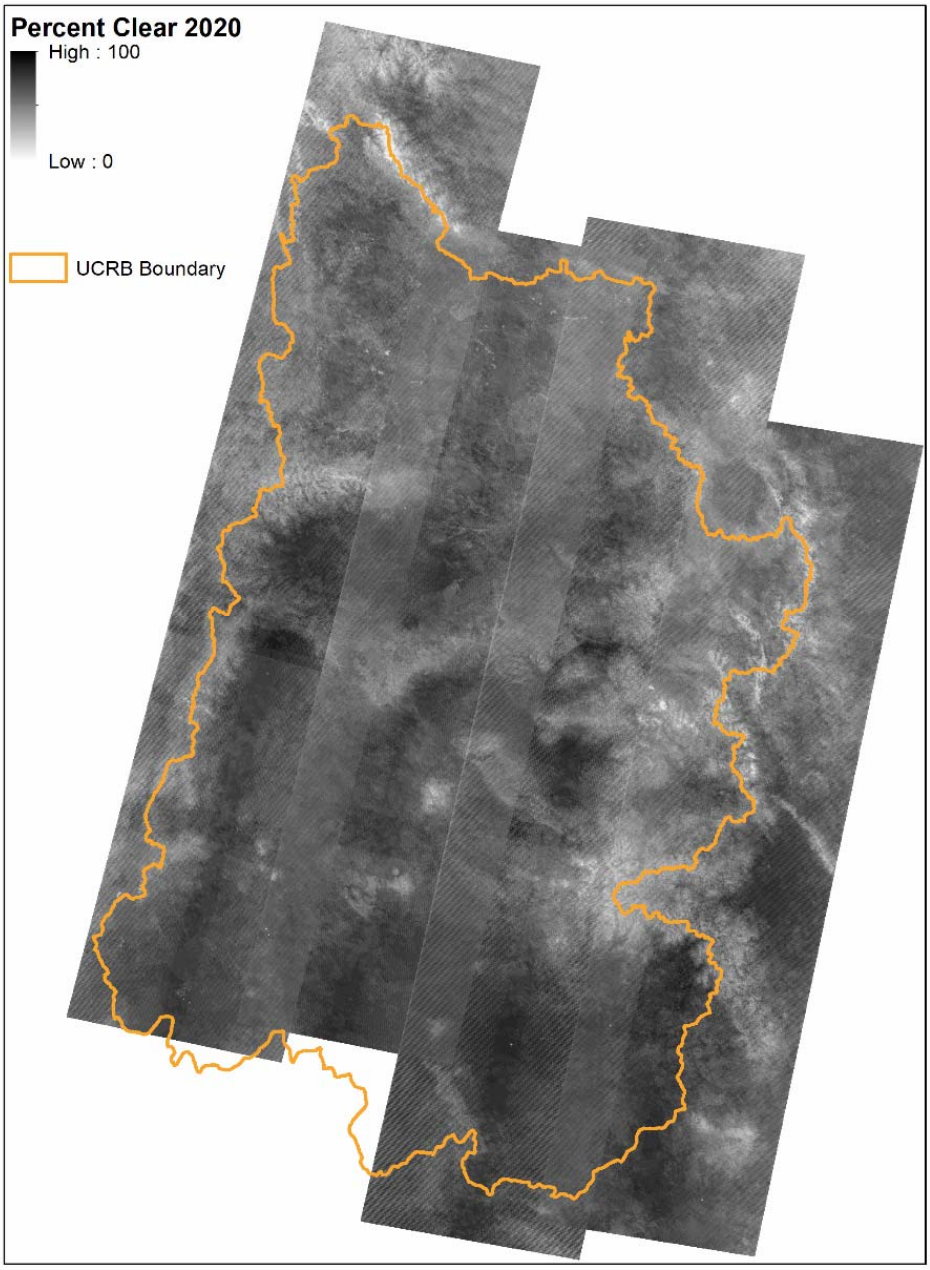

Figure 8. Image showing percentages of clear image dates by pixel (no clouds, no shadows, no SLC-off gaps) across the UCRB for year 2020. Darker intensities indicate more clear image dates for a pixel.

Monthly ET and ET_rF for the months of March-October 2020

Individual satellite images processed using METRIC (Table 1 of Appendix A) were used to establish daily maps of ET_rF for the days of the Landsat images. In addition, synthetic images were produced representing February 2 and November 24, 2020 dates. The synthetic images have full data coverage and

serve as initial and ending points during the interpolation process that require completely filled images. The February 2 image was created by assigning an ET_rF value of 0.4 to the entire image, based on indications of background soil evaporation during those periods from the daily K_e model. The November 24 image was created by assigning an ET_rF value of 0.5 to the entire image, based on indications of background soil evaporation during those periods from the daily K_e model. The values for the synthetic images only impact time periods prior to the first real images that generally occurred in early March and after the last real images that generally occurred in mid-November. Therefore, they had little impact on the monthly ET estimates.

The March, April, May, June, July, August, September and October 2020 monthy ET images were produced by linearly interpolating ET_rF information among individual satellite image dates, for each path, to produce a stacked image containing 245 layers of daily ET_rF covering the March 1 – October 31 time period. The daily ET_rF images tend to follow trends in daily ET caused by vegetation development and evaporation reflecting precipitation events occurring on days immediately before image acquisitions. Following their production, the daily ET_rF images were multiplied by the daily reference ET (ET_r) images originating from bias-corrected GridMet data for each day of the growing season to produce daily ET images. The daily ET were then summed over each month to produce monthly ET. The reference ET_r images account for impacts of weather on daily potential ET demand. Only clear-sky pixels were used for the linear interpolation of daily ET_rF. A python process was used to perform the interpolation.

Description of METRIC Monthly Products

Monthly ET, ET_rF and ET_r

The 2020 ET products consist of several image sets with monthly and metadata information for each path. The monthly ET image data sets have three layers. The first layer is the monthly ET in mm, the second layer is the monthly ET_rF, and the third layer is monthly ET_r in mm. These monthly images have file names starting with "ET" and ending with the month they represent, for example, *ET_P37_2020_04.img* for April of 2020 for the Path 37 multi-row mosaic. The images were produced in ERDAS Imagine *img* format.

Figures 9a-9g show monthly ET and ET_rF for March to October 2020 for the four path coverage of the UCRB following mosaicking of the ET and ET_rF layers over the four Landsat paths. Some seamlines are occasionally visible in the figures where Landsat paths or rows were joined. Small differences in ET_rF across the seamlines was caused by variation in image calibration during the ET_rF production process. Other differences are caused by differences in background evaporation for rainfed areas on the different image dates in two adjacent paths and timing of rainfall prior to the images. Differences among paths and rows are considered to be within the error of the overall METRIC process which is estimated to be about +/-10%.

ET_rF tended to become progressively higher from March through August as irrigated crops developed. ET_rF of rainfed areas at lower elevations tended to become progressively lower through the growing season as soils dried out and sparse vegetation became basically dormant. Higher elevations tended to have sustained ET_rF from forested areas throughout the March – October period with highest levels during late spring and early summer. ET_rF from irrigated areas tended to dominate the landscape during September and October, when natural vegetation was either dry or becoming less active.

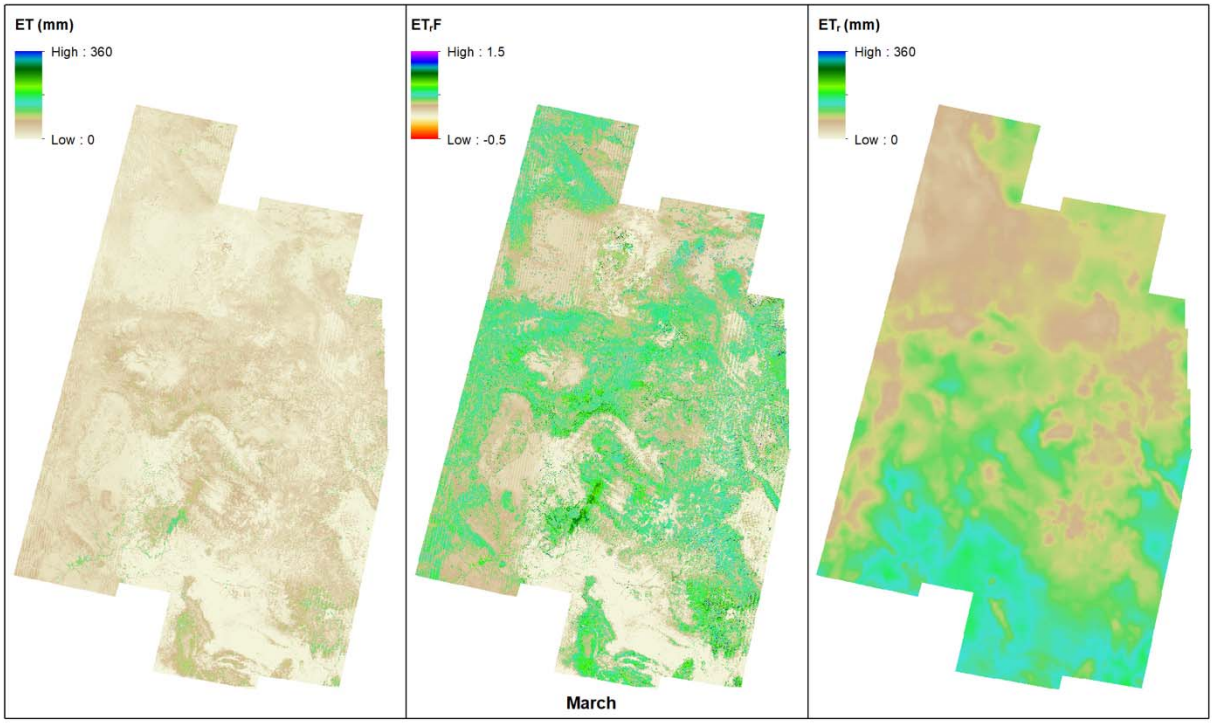

Figure 9a. ET in millimeters (left), ET_rF (center) and alfalfa reference ET_r (right) for the month of March 2020 across the UCRB.

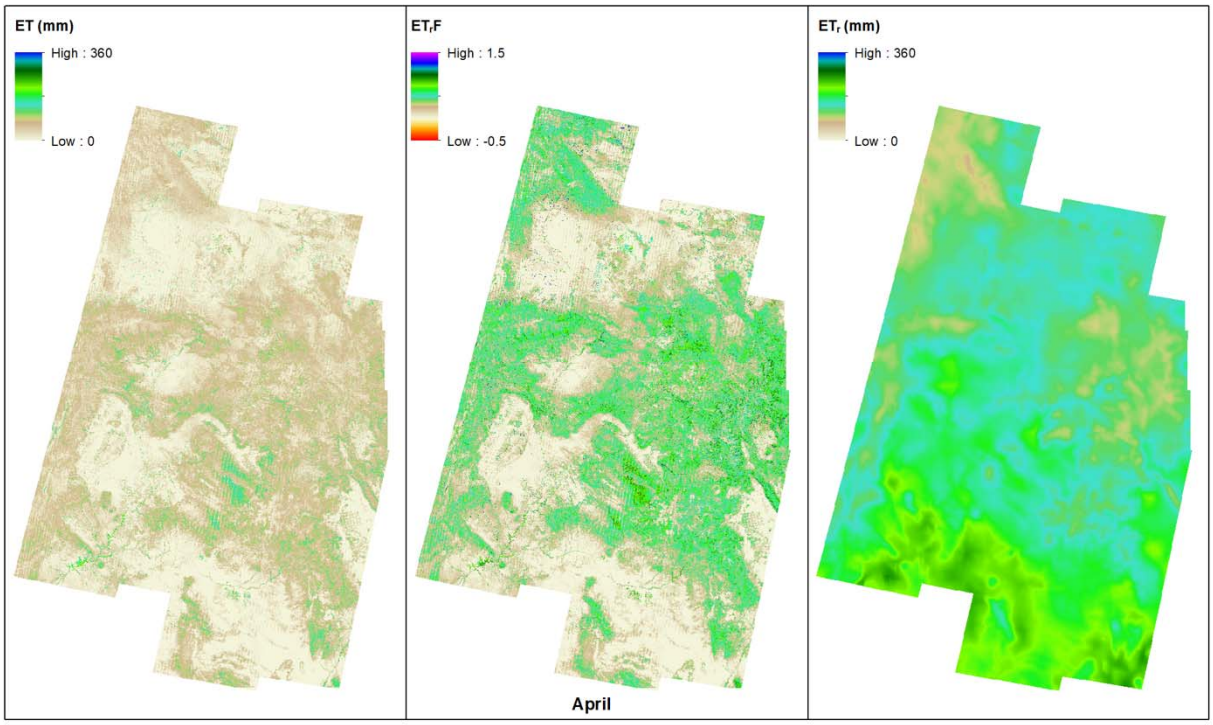

Figure 9b. ET in millimeters (left), ET_rF (center) and alfalfa reference ET_r (right) for the month of April 2020 across the UCRB.

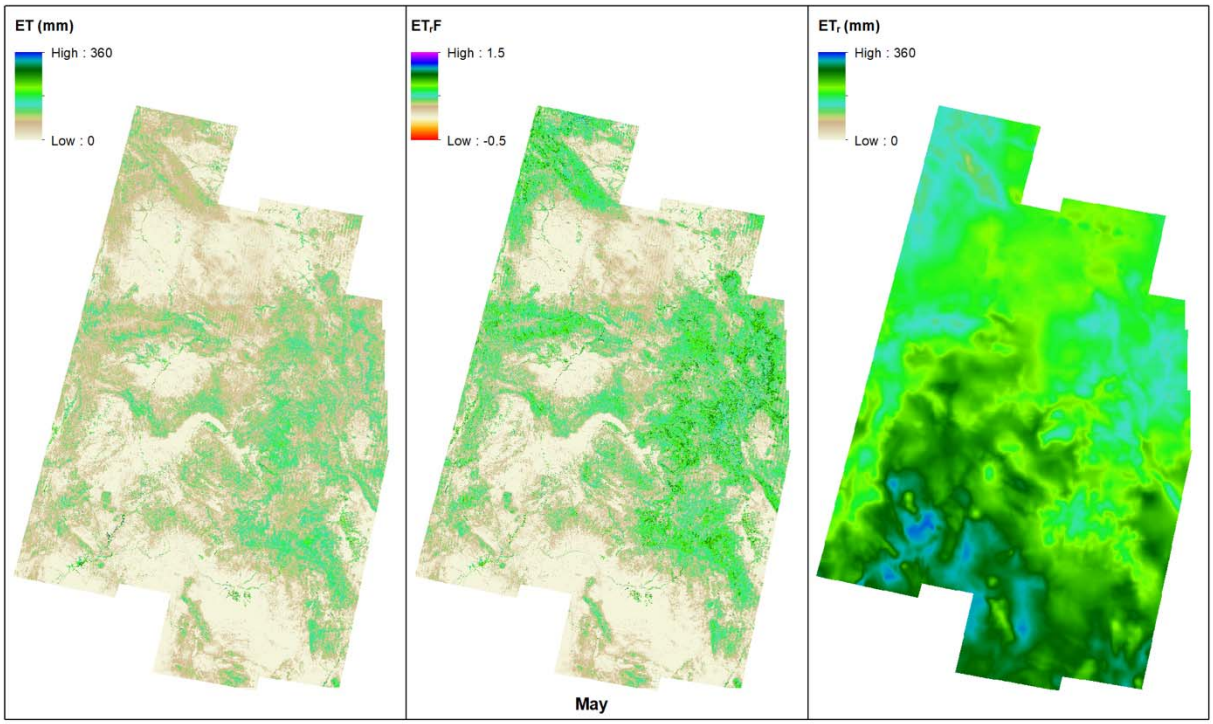

Figure 9c. ET in millimeters (left), ET_rF (center) and alfalfa reference ET_r (right) for the month of May 2020 across the UCRB.

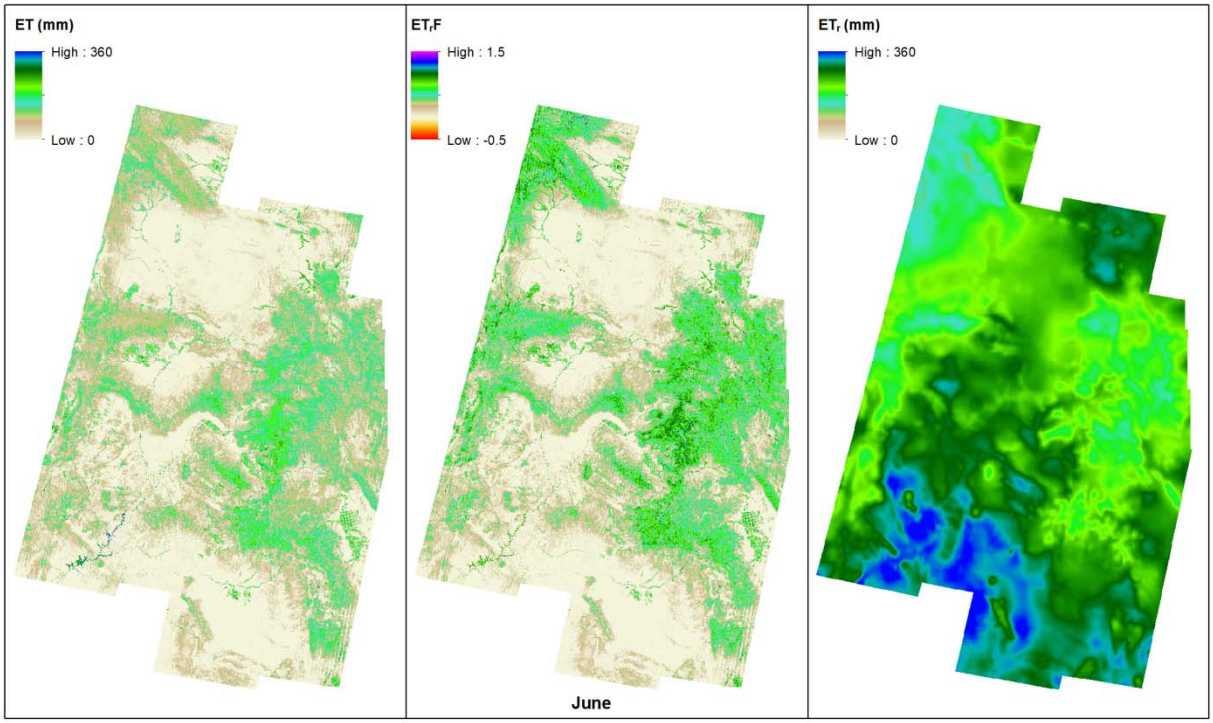

Figure 9d. ET in millimeters (left), ET_rF (center) and alfalfa reference ET_r (right) for the month of June 2020 across the UCRB.

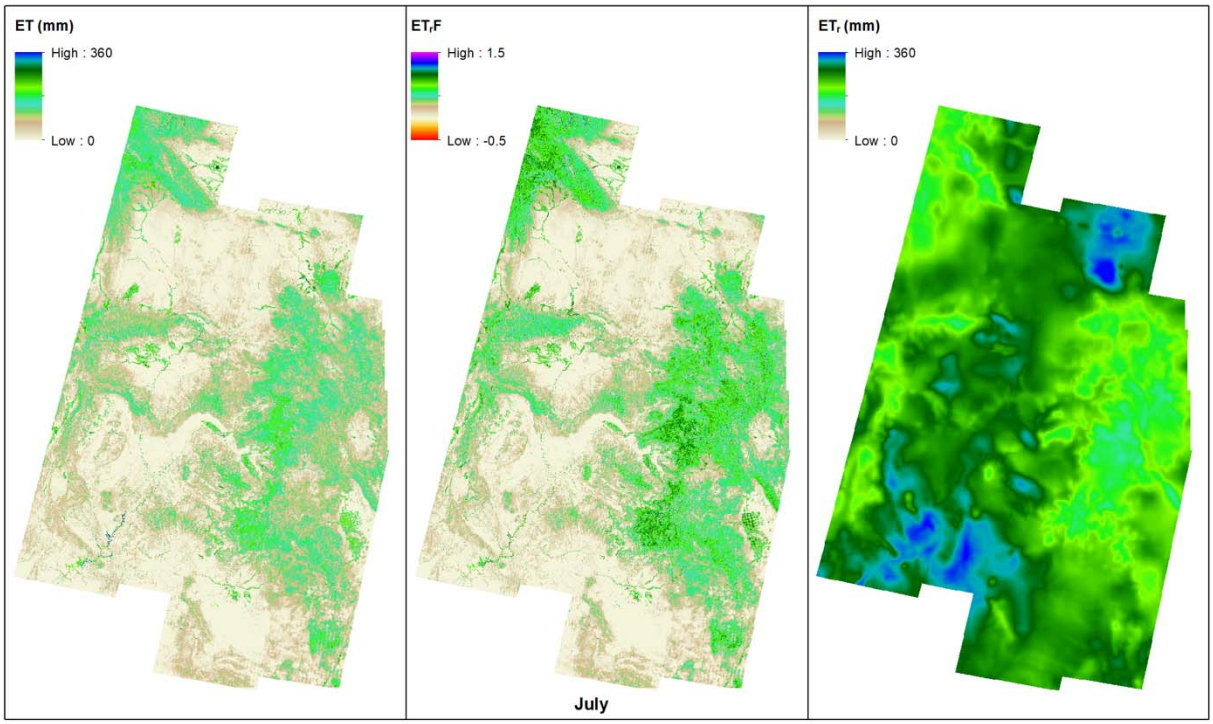

Figure 9e. ET in millimeters (left), ET_rF (center) and alfalfa reference ET_r (right) for the month of July 2020 across the UCRB.

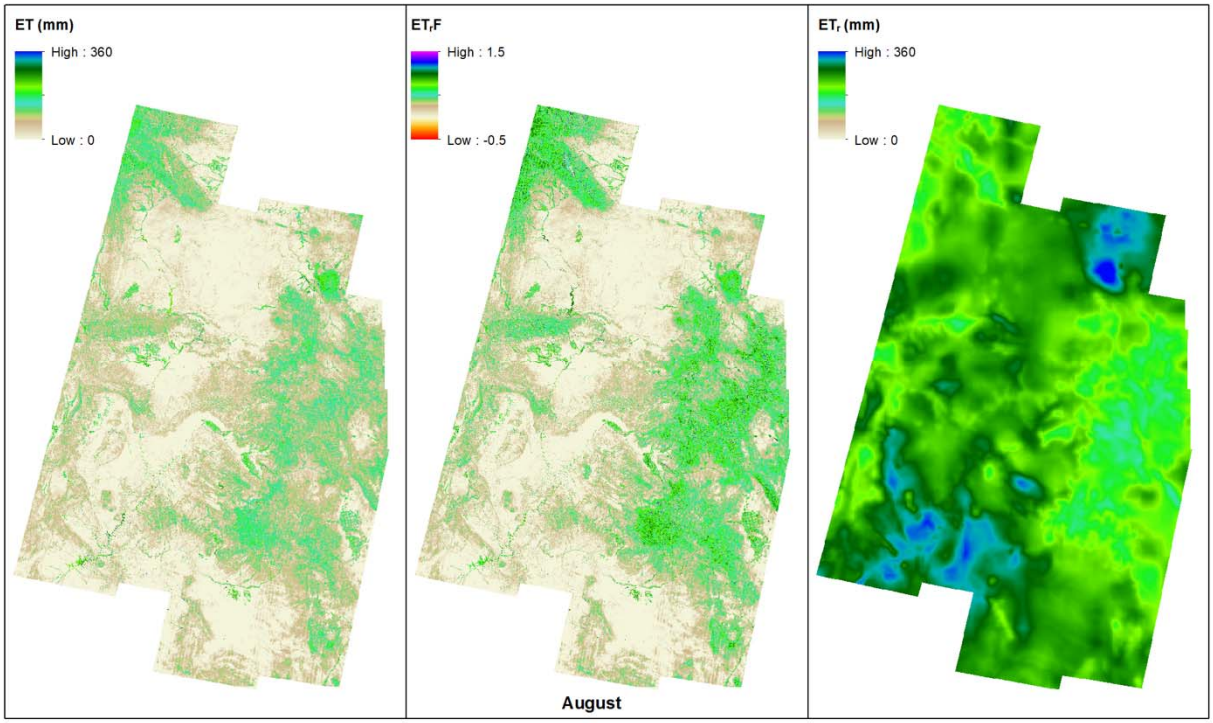

Figure 9f. ET in millimeters (left), ET_rF (center) and alfalfa reference ET_r (right) for the month of August 2020 across the UCRB.

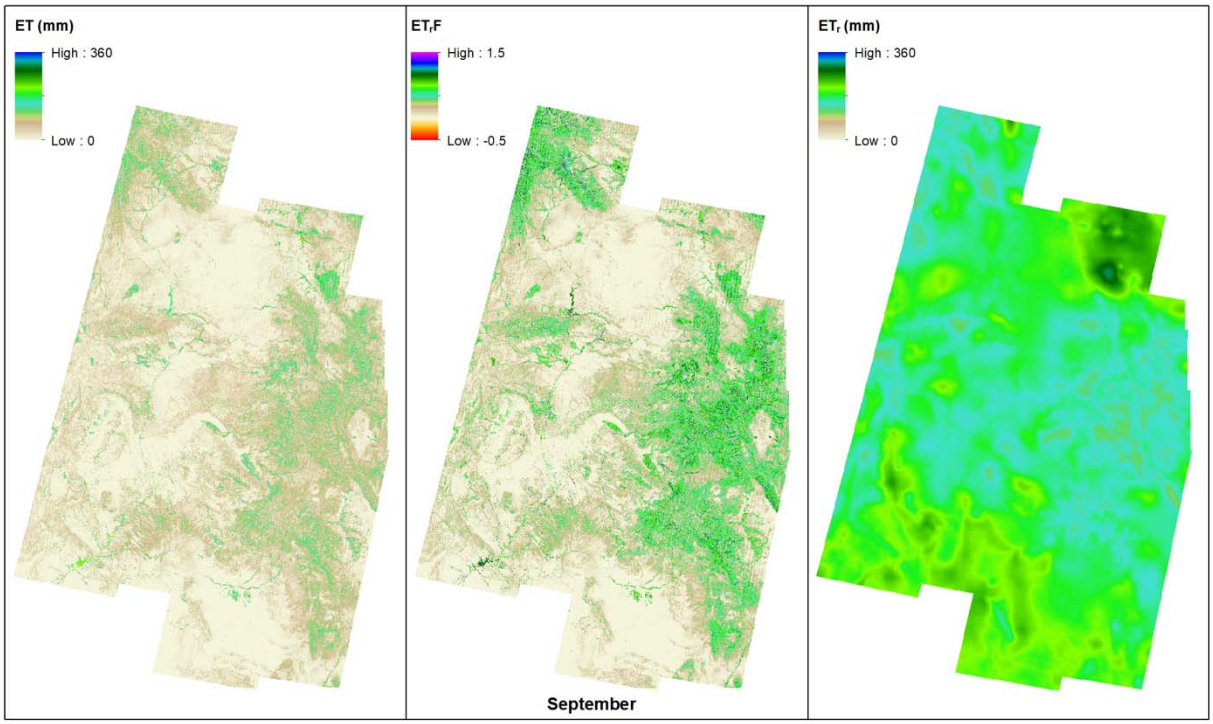

Figure 9g. ET in millimeters (left), ET_rF (center) and alfalfa reference ET_r (right) for the month of September 2020 across the UCRB.

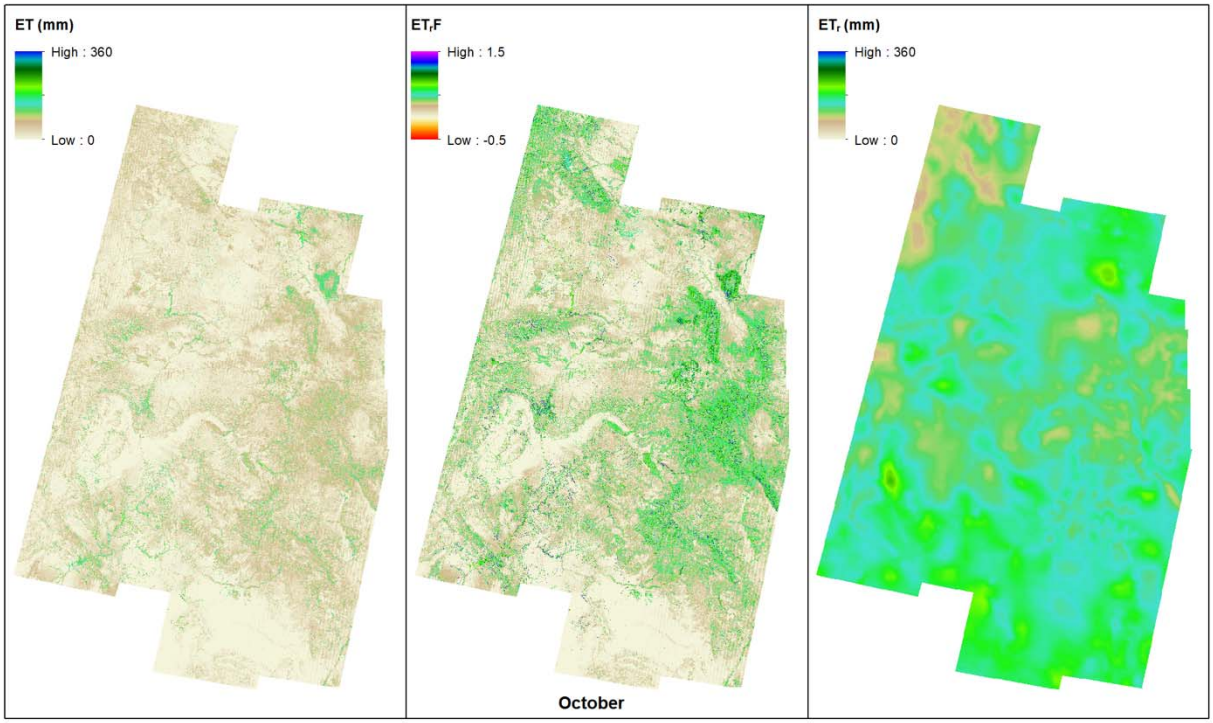

Figure 9h. ET in millimeters (left), ET_rF (center) and alfalfa reference ET_r (right) for the month of October 2020 across the UCRB.

Summary ET and ET_rF for March through October

Growing season summary products were produced for total actual evapotransiration and season-average ET_rF. March-October total ET and March-October season-average ET_rF are shown in figure 10.

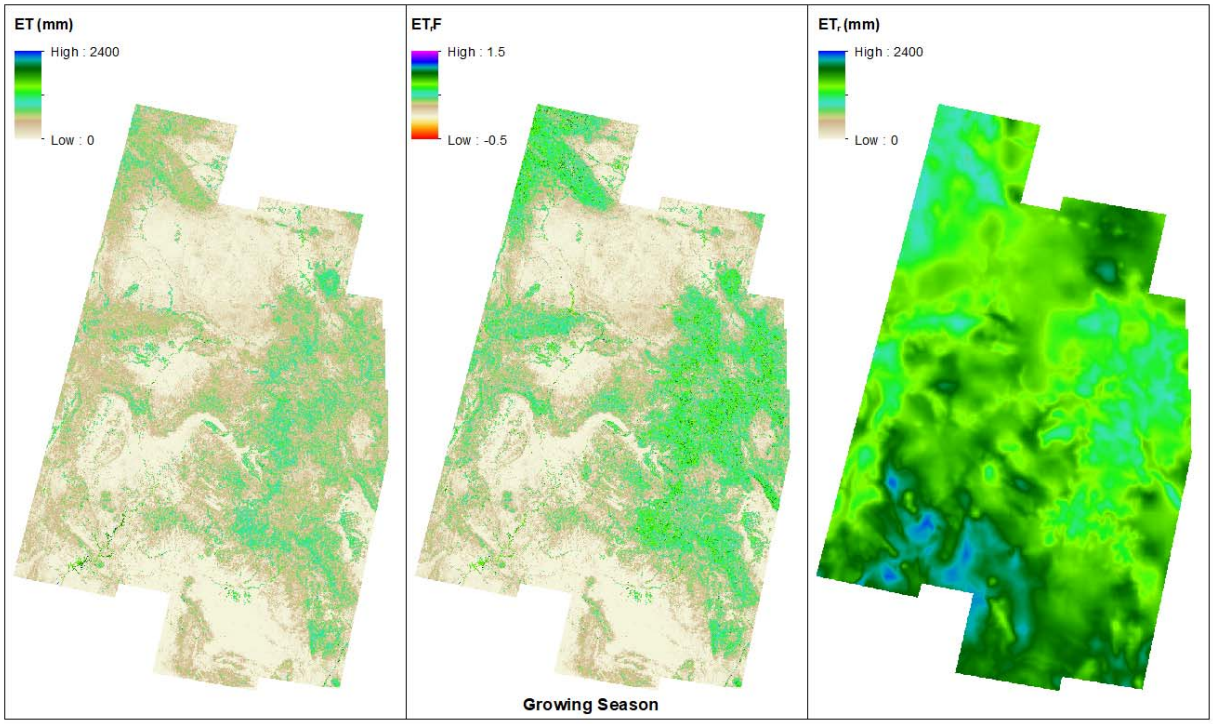

Figure 10. ET in millimeters (left), ET_rF (center) and alfalfa reference ET_r (right) for the March to October growing period for 2020 across the UCRB.

Cloud assessment metadata rasters

A metadata raster is included in products delivered for each Landsat path. The metadata raster describes the cloud assessment for each pixel during the growing season period, as shown earlier in Figure 8. The first layer of the image reports the number of clear images for each pixel during the interpolation period. The second layer reports the number of images where a pixel was cloudy or a Landsat 7 SLC-off gap, and was therefore not used during the interpolation process for the integration period. The raster file names for the cloud assessment begin with the Path number (Path37, for example), and end with ".mask.img".

6. Mosaicing the four paths

Monthly and growing season (March-October) mosaics were produced for the 4-path area covering the Upper Colorado River Basin region as a final step. This final product was produced by mosaicking the multi-layer (ET and ET_rF) images produced for each of the four paths during the time-integration

steps. The mosaicking was done using ERDAS Imagine using a combination of feathering and overlay processes in the path overlap areas. The feathering process applies most weight to the path where the pixel in the overlap area lies furthest from the image edge.

7. Summary

Monthly evapotranspiration (ET) maps were produced for March, April, May, June, July, August, September and October 2020 for the Upper Colorado River basin in addition to March-October and April-October summary images. The products have 30 m spatial resolution and cover Landsat WRS paths 37, 36, 35 and 34. ET was produced using the Google Earth Engine eeMETRIC version of the METRIC model (Mapping Evapotranspiration at high Resolution using Internalized Calibration) developed by the University of Idaho and University of Nebraska-Lincoln partnership. The METRIC procedure utilizes visible, near-infrared and thermal infrared energy spectral bands from Landsat satellite images and weather data to calculate ET on a pixel by pixel basis. Surface energy is partitioned into net incoming radiation (both solar and thermal), ground heat flux, sensible heat flux to the air and latent heat flux. The latent heat flux is calculated as the residual of the energy balance and represents the energy consumed by ET. Reference ET is used to account for day to day impacts of weather on ET demands, with information on individual pixel behavior, relative to the reference ET, provided by the individual Landsat image dates. Evaporation from open water is estimated using an aerodynamic evaporation model rather than from energy balance for increased accuracy.

8. References

Abatzoglou John T., 2013. Development of gridded surface meteorological data for ecological applications and modelling. Int. J. Climatol. 33, 121–131. https://doi.org/10.1002/joc.3413

Allen, R.G. 2011. Skin layer evaporation to account for small precipitation events—An enhancement to the FAO-56 evaporation model. Agricultural Water Management. 99(1):8-18.

Allen, R.G., 2012. REF-ET: Reference Evapotranspiration Calculation Software for FAO and ASCE Standardized Equations. University of Idaho, 82 pp. [http://www.kimberly.uidaho.edu/ref-et/index.html]. Contact author for updates.

Allen, R.G., Pereira, L.S., Raes, D., Smith, M., 1998. Crop Evapotranspiration. Guidelines for computing crop water requirements. FAO Irrig. and Drain. Paper 56. FAO, Rome, 300 pp.

Allen, R.G., Tasumi, M., Trezza, R., 2007a. Satellite-Based Energy Balance for Mapping Evapotranspiration with Internalized Calibration (METRIC) – Model. J. Irrig. Drain Engr., 133(4), 380-394.

Allen, R.G., Tasumi, M., Morse, A., Trezza, R., Wright, J.L., Bastiaanssen, W., Kramber, W., Lorite, I., Robison, C.W., 2007b. Satellite-Based Energy Balance for Mapping Evapotranspiration with Internalized Calibration (METRIC) – Applications. J. Irrig. Drain Engr., 133(4), 395-406.

Allen, R.G., Trezza, R., Tasumi, M., Kjaersgaard, J.H., 2014. METRIC. Mapping Evapotranspiration at High Resolution. Applic. Manual, V 3.0. University of Idaho. 279 pp.

Allen, R.G., J.H. Kjaersgaard, R. Trezza, A. Oliveira, C. Robison, I. Lorite-torres. 2011. Refining components of a satellite based surface energy balance model to complex-land use systems. Proceedings of Remote Sensing and Hydrology 2011 Symposium held at Jackson Hole, Wyoming, USA, September 2011, IAHS Publ. 3XX, 2011. 3 p.

ASCE-EWRI, 2005. The ASCE Standardized Reference Evapotranspiration Equation. ASCE, Reston, Virginia.

Chen, J., X Zhu, JE Vogelmann, F Gao, S Jin, 2011. A simple and effective method for filling gaps in Landsat ETM+ SLC-off images. Remote Sensing of Environment, 1053-64.

Cosgrove, B.A., Lohmann, D., Mitchell, K.E., Houser, P.R., Wood, E.F., Schaake, J.C., ... & Luo, L. 2003. Real-time and retrospective forcing in the North American Land Data Assimilation System (NLDAS) project. Journal of Geophysical Research: Atmospheres, 108(D22).

Jensen, M.E. and R.G. Allen (ed.). 2016. Evaporation, Evapotranspiration and Irrigation Water Requirements. ASCE Manual of Practice no. 70, revised. 744 pages.

Kjaersgaard, J., Allen, R. and Irmak, A., 2011. Improved methods for estimating monthly and growing season ET using METRIC applied to moderate resolution satellite imagery. Hydrological Processes, 25(26), pp.4028-4036.

NLCD (2011): Homer, C.G., Dewitz, J.A., Yang, L., Jin, S., Danielson, P., Xian, G., Coulston, J., Herold, N.D., Wickham, J.D., and Megown, K., 2015, Completion of the 2011 National Land Cover Database for the conterminous United States-Representing a decade of land cover change information. Photogrammetric Engineering and Remote Sensing, v. 81, no. 5, p. 345-354

Wright, J.L., 1982. New evapotranspiration crop coefficients. J. Irrig. Drain. Engr., 108(1), 57-74.

Appendix A. UCRB Monthly ET and ETrF for the months of March-October 2020.

Individual Landsat 7 and 8 satellite images processed using eeMETRIC[1] (METRIC) algorithm on the Google Earth Engine Platform[2] producing ET_rF images for the dates listed in Table A1 through Table A4. The processing domain was paths 34, 35, 36 and 37; and rows 30, 31, 32, 33, 34 and 35. Not all rows were processed for each path as signified by the "blue" highlighted columns in the table. The individual satellite images for each overpass date were initially screened based on clouds present. For some overpass dates the entire set of row images were discarded and the overpass date has been omitted from the tables. The areas highlighted in "grey" indicate that the image for that row on that date considered to be too cloudy.

The eeMETRIC produced ET_rF scenes consisted of four bands: ETrF, NDVI, Buffered Cloud Mask and Landsat 7 SLC gap mask. After downloading the individual scenes, the images were reprojected to the Albers Equal Area projection[3] (AEA) and the layers imported into the appropriate processing tree subfolders as individual images. After re-projection the images were shifted by 15 meters to align with the customized land use map provided by David Eckhart of the USBR for processing in 2018. During the import process, the mask images were converted from float to integer images with any "NaN" values converted to NoData values. To supplement the review of the eeMETRIC ETrF images, the national land use dataset[4] was downloaded and reprojected to the AEA projection used for the Upper Colorado River Basin application.

The eeMETRIC path/row ET_rF images for each over pass date were evaluated by producing scatter plots of ETrF versus NDVI and cumulative frequency distributions of ETrF for various land use classifications (Figure A5). The individual ET_rF path/row images for each overpass were mosaiced together for visual review like that shown in Figure A6. The individual ET_rF images were adjusted based on the example figures and in-depth review of specific fields. The adjustments consisted of adjusting the high and/or low ends of the ETrF values in a linear fashion (Table A1 through Table A4). Using the low- and high-end adjustments for each row in the path for the overpass date, the rows were blended (mosaiced) together to form a single ET_rF image.

Adjustments to the individual eeMETRIC scenes are based on linear stretching of ET_rF between two points and clamping of extreme ET_rF values. For the 2020 processing the clipped range of ET_rF values was -0.05 to 1.50. Adjusted ET_rF values below or above the limits were set to the range limits. The linear end points for the linear stretch were typically 0 and 1 for the low and high ends. The low/high adjustment factors shown in the tables (Table A1 through Table A4). A value of zero (0) means no adjustment at the endpoint. For values below the low endpoint, the low-end adjustment factor was applied without consideration of the high-end adjustment factor. Likewise for value

[1] Allen R, Morton C, Kamble B, Kilic A, Huntington J, Thau D, et al. (2015) EeMETRIC: A Landsat-based evapotranspiration mapping tool on the Google Earth Engine. 2015 ASABE / IA Irrigation symposium: emerging technologies for sustainable irrigation—a tribute to the career of terry howell, Sr Conference Proceedings. St. Joseph, MI: ASABE

[2] Gorelick, N., Hancher, M., Dixon, M., Ilyushchenko, S., Thau, D., & Moore, R. (2017). Google Earth Engine: Planetary-scale geospatial analysis for everyone. Remote Sensing of Environment.

[3] Albers Equal Area project 4 specification string: "+proj=aea +lat_1=36.83333333 +lat_2=42.16666667 +lat_0=34 +lon_0=-109 +x_0=500000 +y_0=0 +datum=NAD83 +units=m +no_defs"

[4] Dewitz, J., 2019, National Land Cover Database (NLCD) 2016 Products: U.S. Geological Survey data release, https://doi.org/10.5066/P96HHBIE

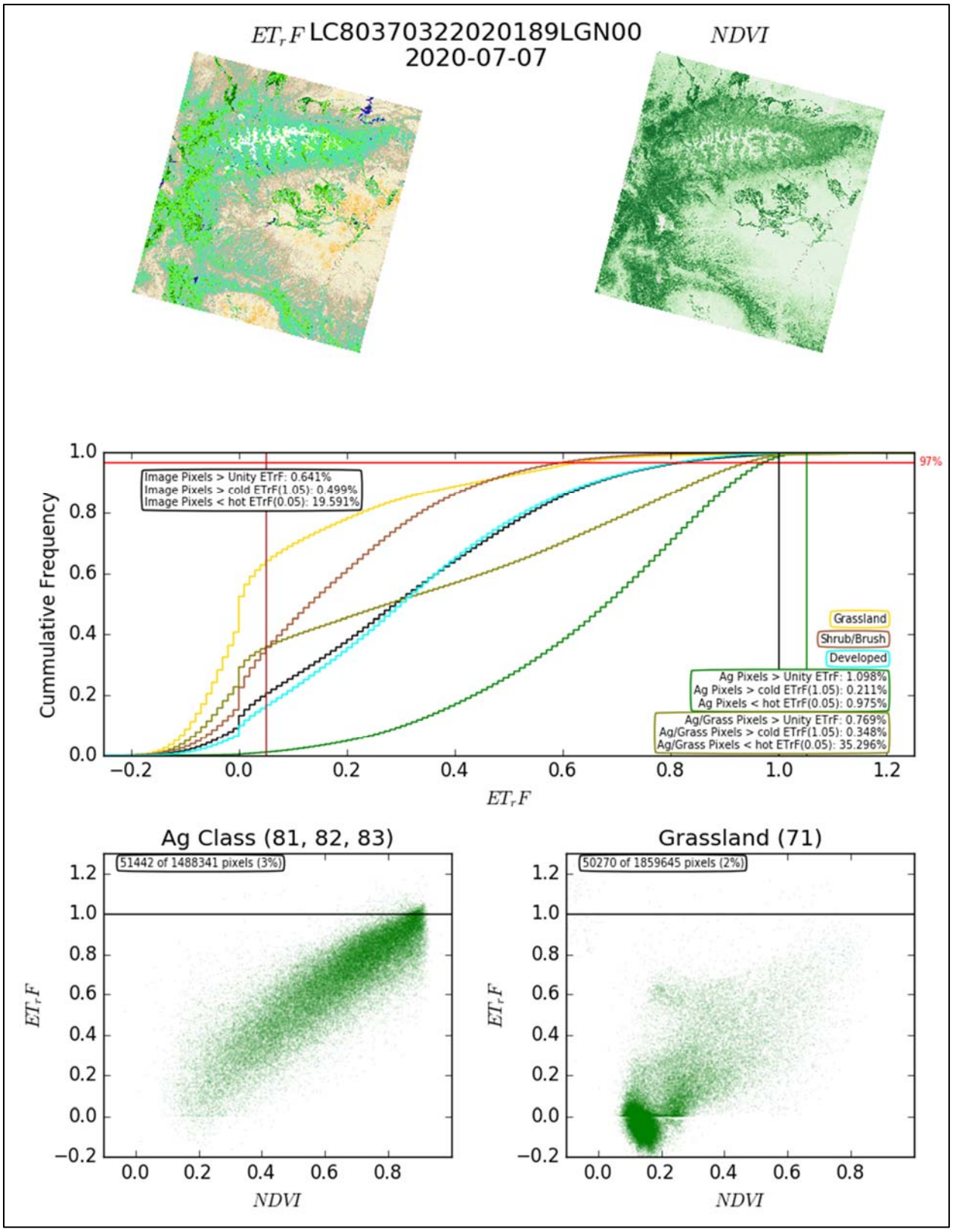

Figure A5. Example evaluation figure for ET_rF based on NDVI and land use classification (July 7, 2020, Landsat 8, Path 37, Row 32.)

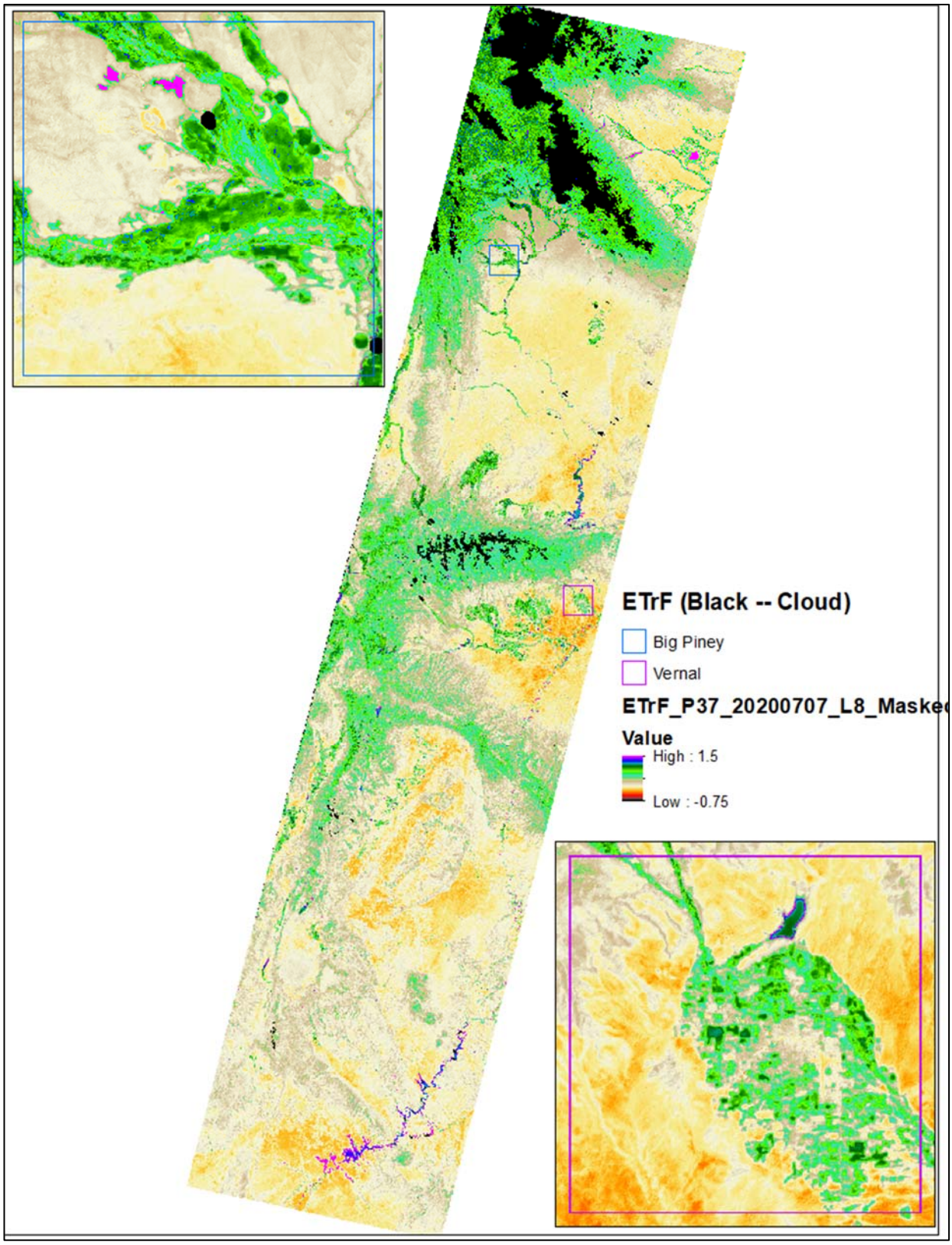

Figure A6. Example mosaiced ET_rF image of a path for and overpass date (July 7, 2020, Landsat 8, Path 37)

Table A1. UCRB 2020 Path 34 Landsat Processing

Upper Colorado River Basin 2020													
Images used in time interpolation and integration for Path 34.													
and adjustments for images													
	Highlights:	Row not included in path				Row not considered.				Row evaluated but not used.			
		Row 30		Row 31		Row 32		Row 33		Row 34		Row 35	
Date	LandSat	LoAdj	HiAdj	LoAdj	HiAdj	LoAdj	HiAdj	LoAdj	HiAdj	LoAdj	HiAdj	LoAdj	HiAdj
2020-01-08	8					0.00	0.00						
2020-01-24	8					0.00	0.00	0.20	-0.20	0.20	-0.20		
2020-02-01	7											0.20	-0.20
2020-02-02	Syn .4	Synthetic constant image with ETrF = 0.4											
2020-02-09	L8									0.00	0.00	0.00	-0.20
2020-02-25	L8											0.20	-0.20
2020-03-04	L7					0.00	0.00	0.00	0.00	0.00	0.00	0.00	0.00
2020-03-28	L8					0.00	-0.20	0.00	0.00	0.00	0.00	0.00	0.00
2020-04-05	L7							0.00	0.00	0.00	0.00	0.00	0.00
2020-04-21	L7					0.00	0.00	0.00	0.00				
2020-04-29	L8					-0.10	-0.05	0.00	0.00	-0.10	0.00	-0.10	-0.15
2020-05-07	L7					0.00	0.00	0.00	0.00	0.00	0.00	0.00	0.00
2020-05-15	L8							0.00	0.00	0.00	0.00	0.00	0.00
2020-05-31	L8					0.00	0.00	-0.10	-0.10	0.00	0.00	0.00	0.00
2020-06-08	L7					0.00	-0.05	0.00	-0.05	-0.15	0.00	0.00	0.00
2020-06-16	L8					-0.10	-0.05	0.00	0.05	-0.10	0.00		
2020-06-24	L7					0.00	0.00	0.00	-0.05	0.00	0.00	0.00	-0.05
2020-07-02	L8					-0.10	0.00	0.00	0.00	-0.05	0.00	0.00	-0.05
2020-07-10	L7					0.00	0.00	0.00	0.00	0.00	0.00	0.00	0.00
2020-07-18	L8					-0.10	0.00	0.00	0.00	-0.10	0.00	-0.10	-0.05
2020-07-26	7					-0.20	0.00					-0.25	-0.05
2020-08-03	L8					-0.20	0.00	-0.10	-0.10	-0.10	-0.10	-0.20	0.00
2020-08-11	L7							0.05	-0.05	0.00	0.00	0.00	0.00
2020-08-19	L8					0.00	0.00	0.00	-0.10	0.00	0.00		
2020-08-27	L7					0.00	0.00	-0.10	-0.15	0.00	-0.05	-0.10	-0.05
2020-09-04	L8					-0.10	0.00	0.00	-0.10	-0.10	0.00	0.00	-0.05
2020-09-12	L7					0.00	-0.05	0.00	0.00	0.00	0.00	-0.20	-0.05
2020-09-20	L8									-0.10	-0.05	0.00	-0.05
2020-09-28	L7					0.00	-0.05	0.10	-0.10	0.05	-0.10	0.05	-0.10
2020-10-06	L8					-0.10	0.00	0.10	-0.05	0.00	-0.10	0.00	-0.15
2020-10-14	L7					0.00	0.00	-0.10	0.00	-0.10	0.00	0.00	0.00
2020-10-30	L7					-0.15	-0.10	-0.10	0.00	0.00	0.00		
2020-11-15	L7							0.00	0.00	-0.10	-0.10	-0.10	-0.25
2020-11-23	L8					0.00	0.00						
2020-11-24	Syn .5	Synthetic constant image with ETrF = 0.5											
2020-12-01	7									0.10	0.00	0.00	0.00
2020-12-09	7					0.00	-0.10	0.00	0.00	0.00	0.00	-0.50	0.00
2020-12-17	7					0.20	0.00						
2020-12-25	8					-0.10	-0.25	0.20	0.00	0.00	-0.25	0.10	0.00

Table A2. UCRB 2020 Path 35 Landsat Processing

Upper Colorado River Basin 2020													
Images used in time interpolation and integration for Path 35.													
and adjustments for images													
	Highlights:	Row not included in path				Row not considered.				Row evaluated but not used.			
		Row 30		Row 31		Row 32		Row 33		Row 34		Row 35	
Date	LandSat	LoAdj	HiAdj	LoAdj	HiAdj	LoAdj	HiAdj	LoAdj	HiAdj	LoAdj	HiAdj	LoAdj	HiAdj
2020-01-07	7					0.00	0.00			0.00	0.00	0.00	0.00
2020-01-15	8			0.20	-0.50	0.20	0.00	0.20	-0.15	0.20	-0.30		
2020-01-23	7									0.20	0.00	0.15	0.00
2020-02-02	Syn.4	Synthetic constant image with ETrF = 0.4											
2020-02-08	L7					0.15	0.00	0.15	0.00	0.15	-0.15	0.00	0.00
2020-02-24	L7							0.10	0.00	0.00	0.00	0.00	0.00
2020-03-03	L8					0.15	0.00	0.15	0.00	0.00	0.00	0.00	-0.10
2020-04-04	L8			0.00	0.00	0.00	-0.15			-0.10	0.00	0.00	0.00
2020-04-12	L7			0.00	0.00			0.00	-0.15				
2020-04-20	L8			0.00	-0.10	0.00	0.00	-0.10	0.00	-0.10	-0.05	-0.10	-0.05
2020-04-28	L7			0.10	0.00	0.00	-0.10	0.00	0.00	0.00	0.00	0.00	-0.05
2020-05-06	L8									-0.20	-0.05	-0.10	0.00
2020-05-14	L7			0.00	-0.25	0.00	-0.15	0.00	-0.10	0.00	0.00	0.00	0.00
2020-05-22	L8			-0.10	0.00	0.00	0.00	0.00	0.00	0.00	0.00	0.00	0.00
2020-05-30	L7			-0.20	-0.05	0.00	0.00						
2020-06-07	L8					0.00	0.10			-0.10	0.05	-0.10	0.00
2020-06-15	L7			-0.15	0.00	0.00	0.00	-0.05	-0.10	0.00	0.00	-0.05	0.05
2020-06-23	L8			-0.20	0.00	-0.05	0.00	-0.05	-0.10	-0.05	-0.05	0.00	0.00
2020-07-01	L7			-0.10	-0.05	0.00	0.00	0.00	0.00	0.00	0.00	0.00	0.00
2020-07-09	L8			-0.10	-0.10	0.00	0.00	0.00	0.00	-0.20	0.00	0.00	0.00
2020-07-17	L7			-0.10	0.00	0.00	0.00	0.00	0.00	-0.05	0.00	0.00	0.00
2020-08-02	L7			-0.10	0.00	0.00	-0.05	0.00	0.00				
2020-08-10	L8			-0.10	-0.05	0.00	-0.05	0.00	0.00				
2020-08-18	L7			0.00	0.00	0.00	0.00	0.00	0.00	0.00	0.00	0.00	0.00
2020-08-26	L8			-0.20	0.00	-0.05	0.00	-0.10	-0.10	-0.10	-0.10	-0.05	0.00
2020-09-03	L7			0.00	0.00	0.00	0.00	0.00	0.00	0.00	-0.10	0.00	0.00
2020-09-11	L8							-0.10	0.00	0.00	0.00	-0.10	0.00
2020-09-19	L7									-0.10	0.00	0.00	0.00
2020-09-27	L8					-0.10	-0.10	0.00	0.00	-0.10	-0.05	-0.15	0.00
2020-10-05	L7			0.00	0.00	-0.05	0.00	0.00	0.00	0.00	0.00	0.00	0.00
2020-10-13	L8			-0.20	0.00	-0.20	0.00	0.00	0.00	0.00	-0.10	-0.10	-0.05
2020-10-21	L7			-0.10	0.00	-0.15	0.00	-0.05	-0.05	-0.10	-0.10	-0.05	-0.10
2020-10-29	L8			-0.10	-0.10	0.00	0.00	-0.30	-0.10	-0.20	-0.30	-0.10	-0.15
2020-11-06	7									0.00	0.00		
2020-11-22	L7			0.00	0.00	0.00	0.00	0.00	0.00				
2020-11-24	Syn .5	Synthetic constant image with ETrF = 0.5											
2020-11-30	8			0.00	0.00	-0.10	-0.10	-0.10	-0.10	-0.10	-0.10	-0.10	-0.25
2020-12-08	7			-0.20	-0.25	0.00	0.00	0.00	0.00	0.00	0.00	0.00	-0.20
2020-12-16	8									0.00	0.00	0.00	0.00
2020-12-24	7			0.20	0.00	0.20	0.00	0.20	0.00	0.00	0.00	0.00	0.00

Table A3. UCRB 2020 Path 36 Landsat Processing

Upper Colorado River Basin 2020													
Images used in time interpolation and integration for Path 36.													
and adjustments for images													
	Highlights:	Row not included in path				Row not considered.				Row evaluated but not used.			
		Row 30		Row 31		Row 32		Row 33		Row 34		Row 35	
Date	LandSat	LoAdj	HiAdj	LoAdj	HiAdj	LoAdj	HiAdj	LoAdj	HiAdj	LoAdj	HiAdj	LoAdj	HiAdj
2020-01-06	8			0.00	-0.50	0.00	-0.50	0.00	-0.50	0.00	-0.50		
2020-01-14	7					0.00	-0.50	0.00	-0.50	0.00	-0.50		
2020-01-22	8									0.00	-0.50		
2020-02-02	Syn.4	Synthetic constant image with ETrF = 0.4											
2020-02-23	L8			0.00	-0.50								
2020-03-02	L7							0.00	0.00	0.00	0.00		
2020-03-10	L8			0.00	-0.30								
2020-03-26	L8							0.00	-0.10	0.00	-0.10		
2020-04-03	L7			0.00	0.00	0.00	0.00	0.00	-0.10	0.00	0.00		
2020-04-11	L8					-0.10	-0.10	-0.10	-0.10	-0.10	-0.10		
2020-04-19	L7					0.00	0.00	-0.20	0.00	0.00	-0.10		
2020-04-27	L8			0.00	0.00	0.00	0.00	0.00	0.00	0.00	0.00		
2020-05-05	L7			0.00	0.20	0.00	0.00	0.00	-0.10	0.00	0.00		
2020-05-13	L8									0.00	0.00		
2020-05-21	L7					0.00	0.10	0.00	0.05	0.00	0.00		
2020-05-29	L8			0.00	0.00	0.00	0.00	0.00	0.00	0.00	0.00		
2020-06-06	7					0.00	0.00			0.00	0.00		
2020-06-14	L8			-0.20	0.00	0.00	0.00	0.00	0.00	0.00	0.00		
2020-06-22	L7			0.00	0.00	0.00	0.00	-0.10	0.00	0.00	0.00		
2020-06-30	L8							-0.20	0.00	0.00	-0.05		
2020-07-08	L7			0.00	0.00	0.00	0.00	0.00	0.00	0.00	0.00		
2020-07-16	L8			-0.15	0.00	0.00	0.05						
2020-07-24	L7			0.00	0.00	0.00	0.10						
2020-08-01	L8			-0.10	0.00	0.00	0.00	-0.20	0.00	-0.10	0.00		
2020-08-09	L7			0.00	0.05	0.00	0.00	-0.10	0.00	0.00	0.00		
2020-08-17	L8			-0.20	0.00	0.00	0.00	-0.10	-0.05	-0.05	0.00		
2020-08-25	L7			0.00	0.05	0.00	0.00	-0.05	0.00	0.00	0.00		
2020-09-02	L8			-0.20	0.00	-0.10	0.00	-0.10	0.00	0.00	0.00		
2020-09-18	L8					0.00	0.00	-0.25	0.00	0.00	0.00		
2020-09-26	7							-0.25	0.00	0.00	0.00		
2020-10-04	L8			-0.05	0.15	0.00	-0.10	-0.20	-0.10	-0.10	0.00		
2020-10-12	L7			0.00	0.00	0.00	0.00	0.00	-0.10	0.00	0.00		
2020-10-20	8							-0.20	0.00				
2020-10-28	L7			0.10	0.00	0.00	-0.10	0.00	0.00	-0.25	-0.20		
2020-11-13	L7			0.00	-0.50	0.00	-0.50	0.00	0.00	0.00	0.00		
2020-11-21	L8			0.00	-0.20	0.00	0.00	-0.15	-0.10				
2020-11-24	Syn .5	Synthetic constant image with ETrF = 0.5											
2020-11-29	7			0.00	0.00	0.00	0.00	0.00	0.00	0.00	0.00		
2020-12-07	8			0.00	0.00	0.00	0.00	0.00	0.00	0.00	0.00		
2020-12-15	7			0.00	0.00	0.00	0.00	0.00	0.00	0.00	0.00		
2020-12-23	8					0.00	0.00			0.00	0.00		

Table A4. UCRB 2020 Path 37 Landsat Processing

Upper Colorado River Basin 2020													
Images used in time interpolation and integration for Path 37.													
and adjustments for images													
	Highlights:	Row not included in path				Row not considered.				Row evaluated but not used.			
		Row 30		Row 31		Row 32		Row 33		Row 34		Row 35	
Date	LandSat	LoAdj	HiAdj	LoAdj	HiAdj	LoAdj	HiAdj	LoAdj	HiAdj	LoAdj	HiAdj	LoAdj	HiAdj
2020-01-13	8	0.00	0.00	0.00	0.00	0.00	0.00	0.00	0.00	0.00	0.00		
2020-01-29	8	0.00	0.00	0.00	0.00	0.00	0.00			0.00	0.00		
2020-02-02	Syn.4	Synthetic constant image with ETrF = 0.4											
2020-02-14	8			0.00	0.00	0.00	0.00	0.00	0.00				
2020-02-22	7	0.00	0.00	0.00	0.00								
2020-03-01	8									0.00	0.00		
2020-03-17	8	0.00	0.00	0.00	0.00					0.00	0.00		
2020-03-25	7									0.00	0.00		
2020-04-02	L8			0.00	0.00	0.00	0.00	0.20	-0.20				
2020-04-10	L7	0.00	0.00	0.00	0.00	0.20	0.00	0.00	0.00	0.20	0.00		
2020-04-18	L8	0.00	0.00	0.00	0.00					0.00	0.50		
2020-04-26	L7					0.00	0.00						
2020-05-04	L8	0.00	-0.20	0.00	0.00	0.00	-0.10	0.00	0.00	0.10	0.00		
2020-05-12	L7					0.00	-0.10	0.00	0.00	0.00	0.00		
2020-05-20	L8	0.00	0.00			0.00	0.00	0.00	0.00	0.00	0.00		
2020-05-28	L7	0.10	0.00	0.00	-0.10	0.00	0.05	0.00	0.00	0.00	0.00		
2020-06-05	L8	0.00	0.10	0.00	0.10	0.00	0.10	0.00	0.10				
2020-06-13	L7	0.05	0.05	0.00	0.00	0.00	0.05			0.00	0.00		
2020-06-21	L8					0.00	0.10	0.00	0.00	0.00	0.00		
2020-07-07	L8	-0.10	0.10	-0.10	0.00	-0.10	0.05	0.00	0.10	0.00	0.05		
2020-07-15	L7	0.00	-0.05	0.00	0.00	0.00	0.00	0.00	0.00	0.00	0.00		
2020-07-23	L8	-0.10	0.00	0.00	0.00	0.00	0.00	0.00	0.00				
2020-07-31	L7	0.00	0.00	0.00	0.00	0.00	0.00	0.00	0.00	0.00	0.00		
2020-08-08	L8	-0.10	0.10	-0.10	0.00	0.00	-0.05	0.00	0.00	-0.10	0.10		
2020-08-16	L7	0.00	-0.10	0.00	-0.10	0.00	0.00	0.00	-0.10	0.00	0.00		
2020-08-24	L8	-0.10	-0.10	0.00	0.00			0.00	0.00	0.00	0.00		
2020-09-01	L7	-0.10	-0.05	0.00	0.00	0.00	0.00	0.00	0.00	0.00	0.00		
2020-09-09	L8	0.00	0.00	0.00	-0.15	0.00	0.00						
2020-09-17	L7	0.00	0.15	0.00	0.15	0.00	0.00	0.00	0.00	0.00	0.00		
2020-09-25	L8			-0.10	-0.15	0.00	-0.15	0.00	0.00	0.00	0.00		
2020-10-03	L7	-0.10	-0.10	-0.10	-0.20	-0.05	-0.05	-0.05	0.00	0.00	0.00		
2020-10-11	L8	0.00	0.00	0.00	-0.20	0.00	-0.20			0.00	0.00		
2020-10-19	7									0.00	0.10		
2020-10-27	L8	0.00	-0.60					-0.20	-0.20	0.00	0.00		
2020-11-04	L7	0.00	-0.50	0.00	-0.50	-0.10	0.00	0.00	0.10	0.00	-0.50		
2020-11-20	L7	0.00	-0.50	0.00	-0.50	0.00	-0.50						
2020-11-24	Syn .5	Synthetic constant image with ETrF = 0.5											
2020-11-28	8	0.00	-0.60	0.00	0.00	0.00	-0.30	0.00	-0.30	0.00	-0.50		
2020-12-06	7	0.00	-0.60	0.00	-0.60	0.00	-0.60	0.00	-0.60	0.00	-0.60		
2020-12-22	7									0.00	-0.60		

exceeding the high endpoint, the high end adjustment was applied without consideration of the low end. Between the two end points the adjustment factors were applied in weighted method.

$$\widehat{ETrF} = ETrF + \frac{(ETrF - lo_p) * hi_a + (hi_p - ETrF) * lo_a}{(hi_p - lo_p)}$$

where: $\widehat{ETrF}$ is the adjusted ETrF between the endpoints
ETrF is the original ETrF from eeMETRIC
lo_p is the ETrF of the low endpoint
lo_a is the low-end adjustment for ETrF
hi_p is the ETrF of the high endpoint
hi_a is the high-end adjustment for ETrF

Thus, for eeMETRIC scenes in path 36 on June 30th row 33 and 34 (Table A3) the adjustment factors resulted in; the following equations:

Row 33: ETrF + ((ETrF - 0)*0 + (1 - ETrF)*-0.20)/(1-0)
Row 34: ETrF + ((ETrF - 0)*-0.05 + (1 - ETrF)*0)/(1-0)

After application of adjustment factors each eeMETRIC scene was mosaiced together creating a single ET_rF image for an overpass date. Adjoining scenes overlap areas were construct by blending (feathering) the two scenes together. If a scene was missing, the scene area was treated as being completely cloudy. The ET_rF path mosaic for the overpass date was then cloud/shadow/gap mask applied.

The mosaiced overpass images for a path were examined to find the spatial intersection of all the images resulting in a region for interpolation. For each image, the area outside the region was set as missing. The interpolation procedure requires a cloud/shadow/gap free image to produce daily ET_rF images. For interpolation two synthetic images were constructed for the interpolation starting and ending images. The beginning synthetic image was a constant value, 0.4, with a date of February 2nd. The ending synthetic image was a constant value, 0.5, with a date of November 24th. The daily ET_rF interpolation procedure imposes limits on ET_rF occurring in the mosaiced adjusted eeMETRIC images to be in the range of -0.05 to 1.50. Values outside the range are set as being cloud/shadow/gap pixel. For the UCRB 2020 application, the adjustment procedure already imposed the limitation. The actual interpolation period was from March 1st through October 31st using linear interpolation between image dates. The result is a stacked raster of daily ETrF between March 1st and October 31st.

The interpolated daily ET_rF stack was combined with daily reference evapotranspiration (ET_r) to estimate daily ET from which monthly and seasonal ET summaries were produced. The ET_r data set used was supplied by DRI and bias corrected. For the entire paths and subareas (EC tower locations), monthly and seasonal ET, ET_rF and ET_r summaries were computed. The monthly and ET and ET_r summary was the sum of the daily ET (ET_rF * ET_r) and ET_r for the summary period. The negative summary ET values were set to zero. The summary ET_rF was computed as the ratio of the summary ET to the summary ET_r. The daily ET was saved for the subareas (EC tower locations). The path summaries were adjusted for water bodies (as defined by the NLCD) due a wind threshold issue with eeMETRIC resulting in water ET_rF monthly values close to 1.5 for several months. The water body ET and ET_rF was adjusted by multiplying by 0.7 in the monthly product and seasonal recomputed from the adjusted monthly product.

Description of eeMETRIC Products

Monthly and Seasonal ET, ET_rF and ET_r Products

The 2020 ET products consist of several image sets with monthly and seasonal information for each path. The ET product image data sets have three layers. The first layer is the monthly/seasonal ET in mm, the second layer is the monthly/seasonal ET_rF, and the third layer is monthly/seasonal ET_r (alfalfa reference) in mm. These images have file names starting with "*P##"* and ending with the month they represent followed by "*mm_WB*", for example the path 37 April 2020 product name is: *P37_ET_04_WB.img*. The month is replaced by "*GS*" for the seasonal product and represents the period from March through April. The images were produced in the ERDAS Imagine *img* format. For the eddy covariance sites: Big Piney, Vernal, Palisades and Bloomfield; there are 2020 monthly and seasonal ET subarea products for the 20 km area around the site. These products have names with "*BP, VU, PC and BN*" abbreviation between "ET" and the month.

The monthly and seasonal products for paths 34 through 37 were mosaiced together to form a single ET product image over the UCRB application area for each month and seasonal. The image file names have the form "*UCRB_2020_mm*" where is the month, ie, 04 or GS for the seasonal product.

Daily ET_rF and ET Products for Eddy Covariance Locations

For the eddy covariance locations subareas in each path, daily ET and ET_rF were saved for the 20 km area. These rasters are multilayer rasters with each layer representing one day. March 1st 2020 is layer 1 and October 31st 2020 is layer 245. The rasters are named with path, parameter, and subarea information: "*P##_parm_ec.img*" where ## is the path number, parm is ET for ET (mm/day) or ET_rF and *ec* is one of the four subarea abbreviations (BP, VU, PC, BN). These daily images can be sampled to show daily ET/ETrF at pixel(s) in the subarea.

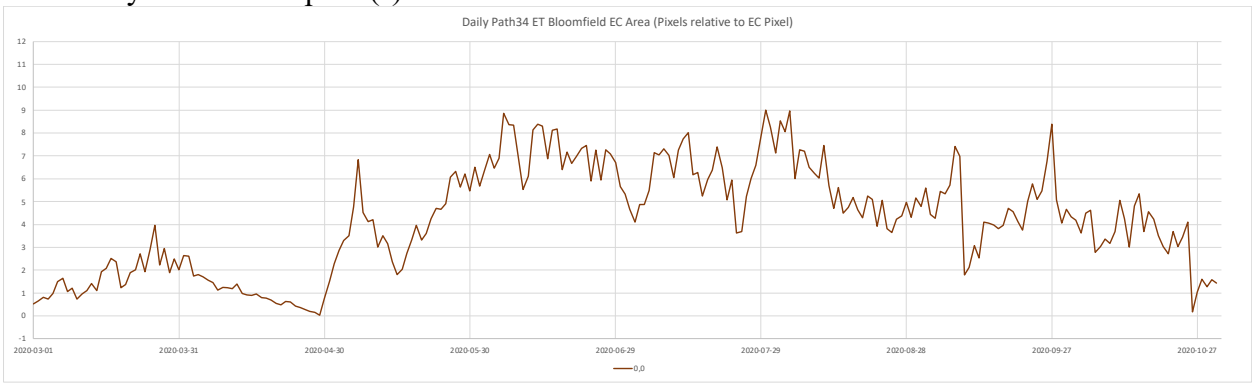

Figure 7. Example daily ET associated with the Path 34 eeMETRIC processing at the Bloomfield eddy covariance location for 2020.

Appendix B. Post-Processing Tasks with eeMETRIC

Following the processing of ETF with eeMETRIC on the Google Earth Engine, additional processing was applied to produce the final monthly ET products. The following describes the steps used.

The 2020 eeMETRIC ET_rF and NDVI images were downloaded from Google Earth Engine separately and had different dimensions and geographic transformations. In addition, the ET_rF scene image had NaN's for any pixel that did not have an ET_rF value due to the pixel being a) outside the scene footprint, b) a cloud/shadow, or in the case of Landsat 7, c) a SLC gap.

To identify clouds and shadows and eventually Landsat SLC gaps, the EROS Landsat BQA image was downloaded from the public access area hosted by Google. To download the corresponding BQA images, the Landsat product identification was required. To obtain the product identifications, the metadata for Landsat imagery over paths 34 through 37, rows 30 through 35 was downloaded from EROS Earthexplorer. The metadata allowed conversion of an entity ID into a product ID. Using that product ID, the BQA images were downloaded for each ETrF scene and used in determining cloud/shadow masks. The following table gives an example of an entity ID vs. a product ID.

Table B.1. Example of an entity ID vs. a product ID

	Entity ID	Product ID
Landsat 7	LE70370302020178EDC00	LE07_L1TP_037030_20200627_20200723_01_T1
Landsat 8	LC80370342020170LGN00	LC08_L1TP_037034_20200619_20200703_01_T1

To coordinate the separate images for ET_rF, NDVI and BQA images, a Python script developed n 2020 was used to import and reproject the images into the processing tree (*PROJECT/PATH/DATE/ORGS*). Another script developed in 2020 was used to take the imported images and clip them to a common area having identical raster dimensions and geotransform, and save them into the processing tree similar to the 2018 application (*PROJECT/PATH/DATE/PARTS*). This script also created the MosaicControl worksheet for later stretching (adjusting) individual ET_rF scenes. The format of the control sheet had been modified from 2018 to identify ET_rF, NDVI and mask file descriptors relative to the project folder instead of a full file descriptor which, in 2018, included the drive designation.

ET_rF images were reviewed by scene by R. Allen using plots of sampled ET_rF vs. NDVI as shown in Figures A1 and B1 to note behavior and relative values at the upper and lower extremes of ET_rF. Colorized images of ET_rF were also reviewed for each scene and date to note spatial trends in ET_rF and to confirm the proposed calibration adjustments. An example of the plots generated by a Python script is shown in Figure B1. Proposed adjustment to that July 7, 2020 date was 0.0 for the lower end of ET_rF and +0.05 for the upper end of ET_rF.

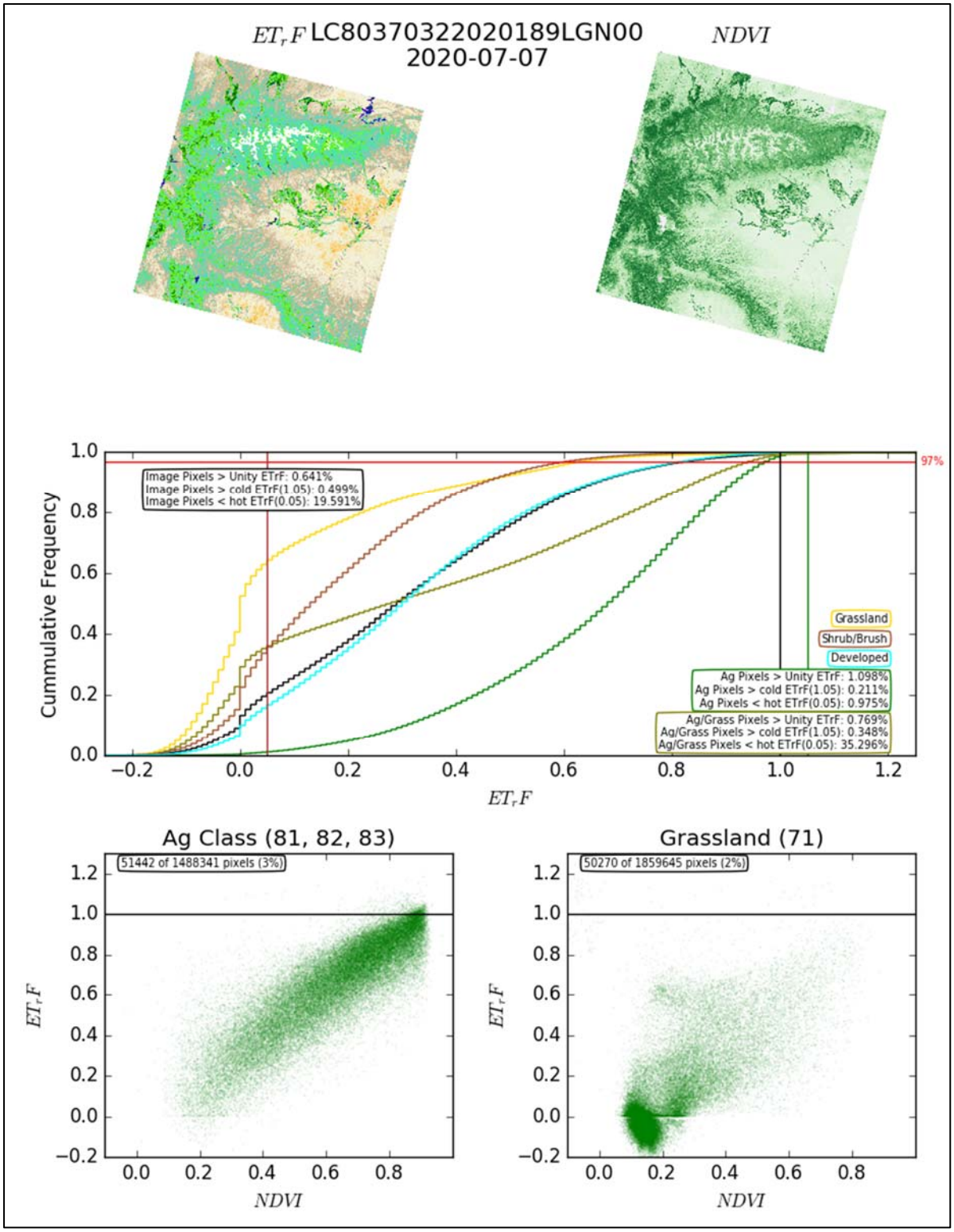

Figure B.1. Example plot of ET_rF vs. NDVI for the July 7, 2020 Landsat 8 image over Path 37 Row 34 showing results for agricultural pixels (lower left) and for grassland land cover (lower right). Also shown is a cumulative frequency plot for ET_rF values for selected land use classes.

Each ET_rF image was opened in an ERDAS Imagine viewer and visually scanned to evaluate adherence of ET_rF values for high NDVI and low NDVI conditions to expected values. For most images, some adjustment was recommended to the high end of ET_rF or low end of ET_rF or both. That adjustment was made by specifying a positive or negative additive at each end of the ET_rF spectrum and adjusting all ETrF values in proportion to their numerical distance from each end point value, which were set to 0.0 and 1.0. A similar procedure is used in the web-based EEFlux application.

Figures B.2 – B.5 show summaries of adjustments at the upper and lower ends for each of the four paths. Recommended adjustments to the upper end of ET_rF were greater in magnitude during winter, early spring and late fall months when the automated calibration procedure of eeMETRIC tended to overstate ET_rF values due to lower thermal contrasts in images and smaller populations of highly vegetated fields. During summer, adjustments ranged from about +0.05 to -0.10. Adjustments to the upper end were generally negative, meaning that ET_rF was lowered. Adjustments tended to be small and less frequent for the lower end of ET_rF.

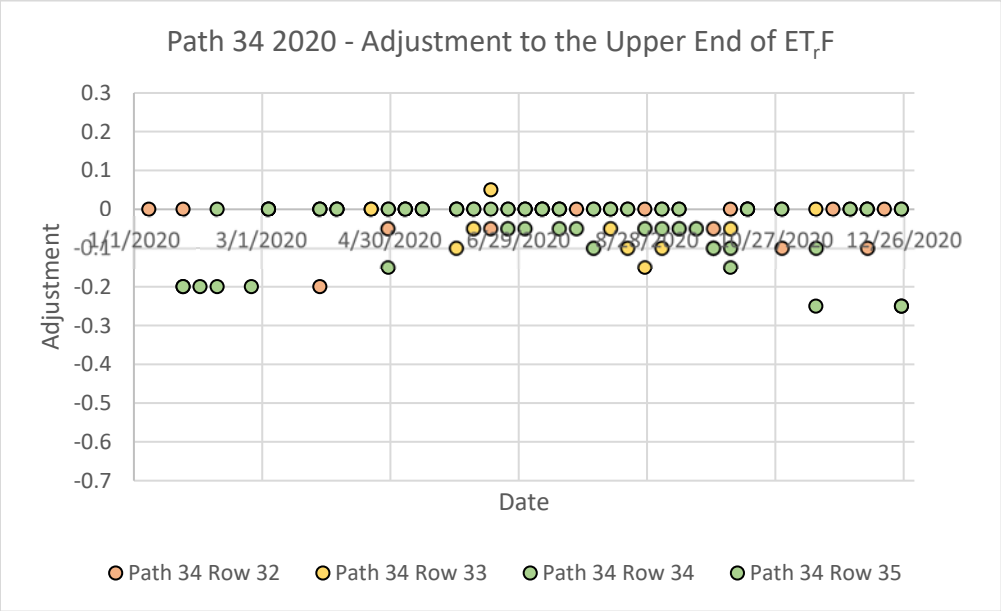

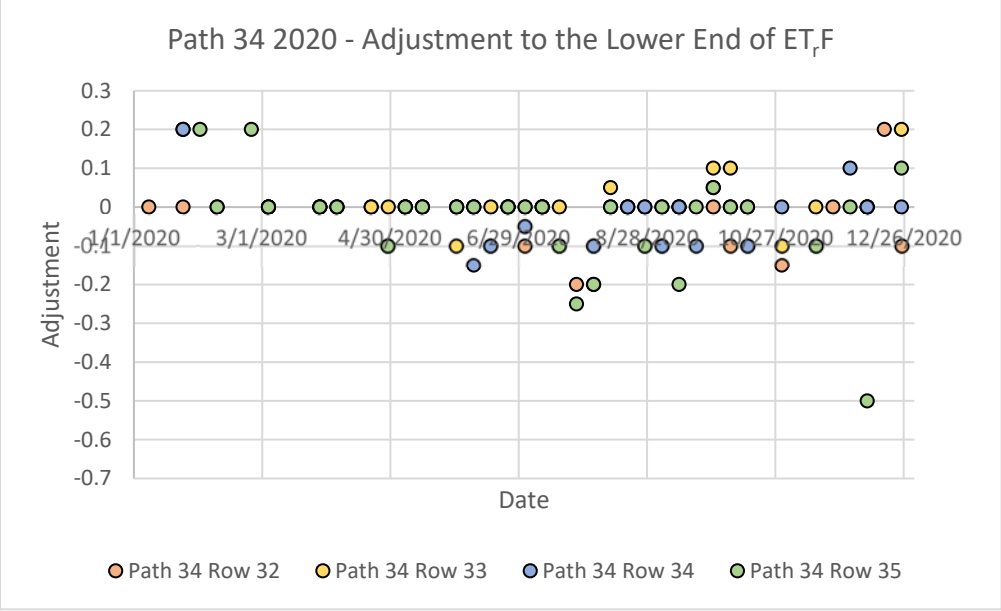

Figure B.2. Summary of additive adjustments at the upper and lower ends of ETrF by image month (one symbol per path/row scene) for Path 34 during 2020.

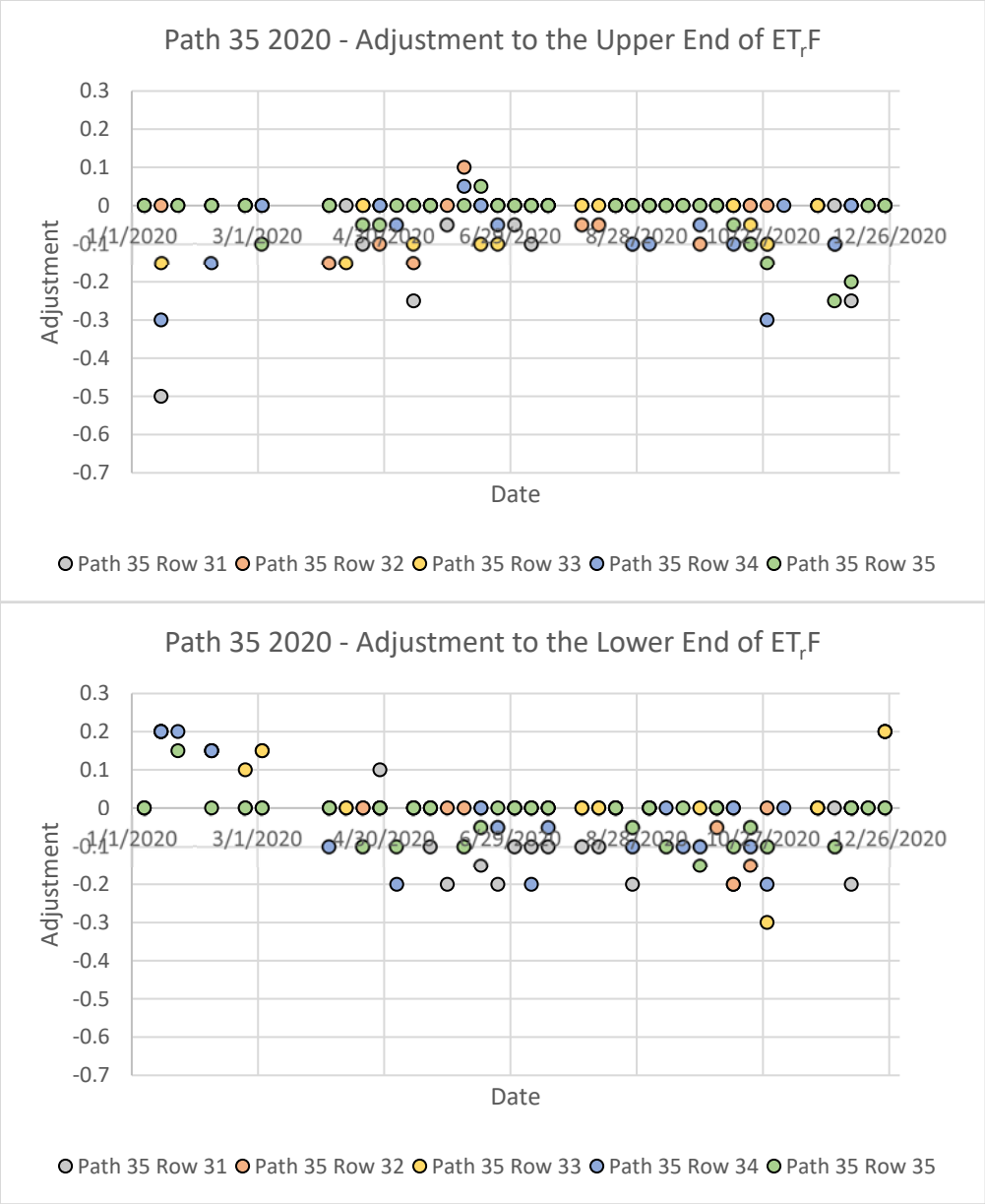

Figure B.3. Summary of additive adjustments at the upper and lower ends of ETrF by image month (one symbol per path/row scene) for Path 35 during 2020.

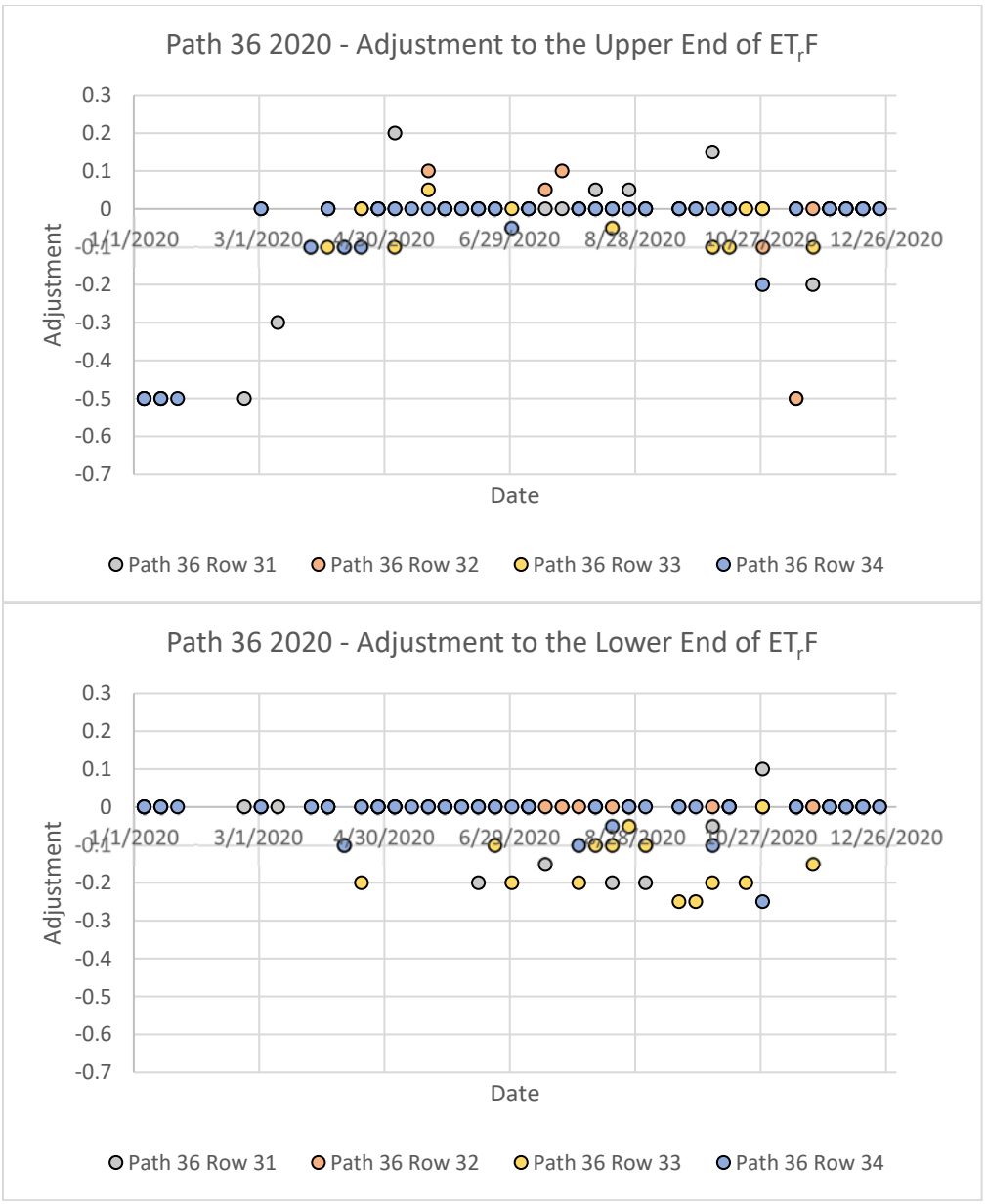

Figure B.4. Summary of additive adjustments at the upper and lower ends of ETrF by image month (one symbol per path/row scene) for Path 36 during 2020.

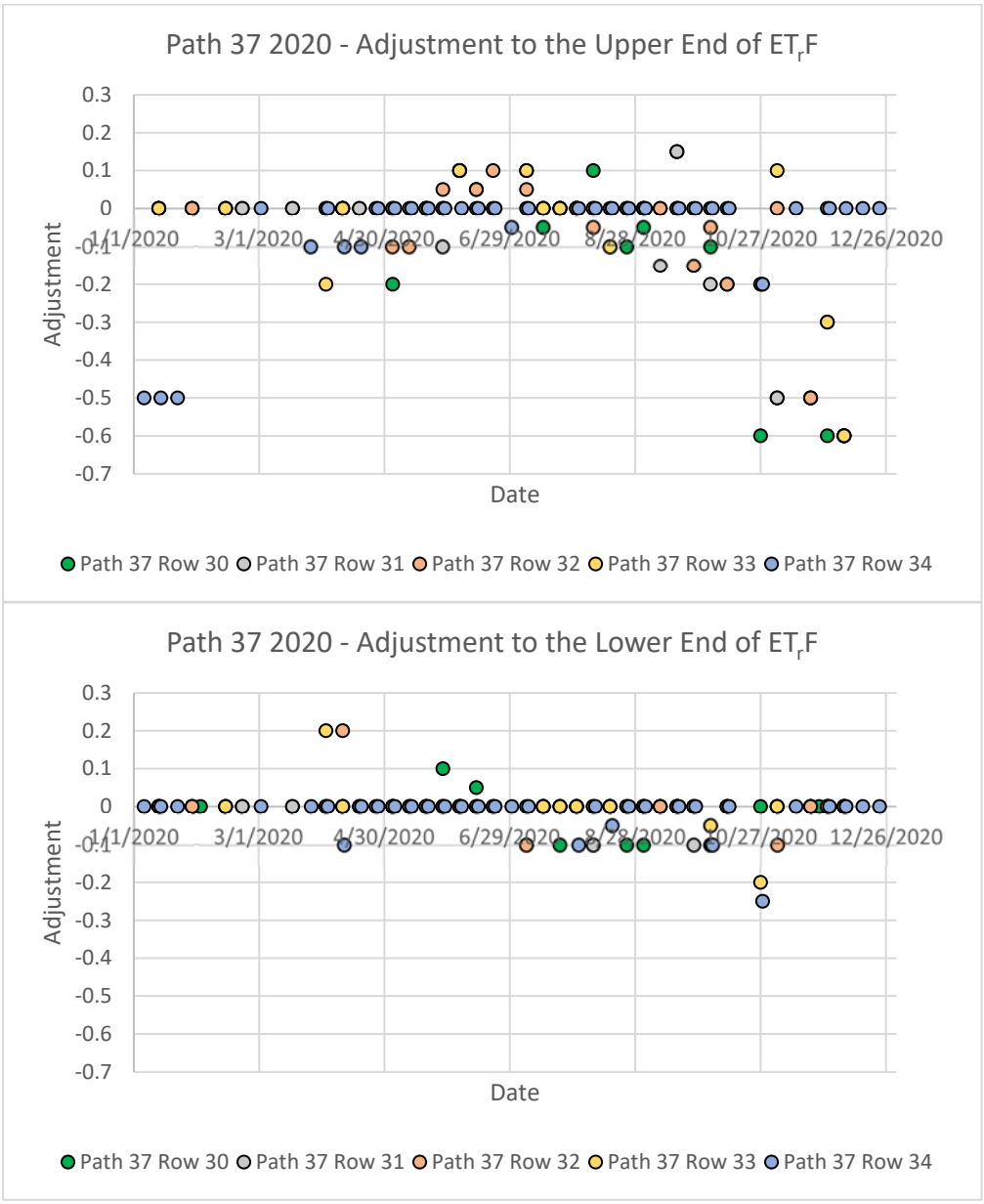

Figure B.5. Summary of additive adjustments at the upper and lower ends of ETrF by image month (one symbol per path/row scene) for Path 37 during 2020.

The interpolation/integration AOI's were used from the 2018 application after review. Path 34 was an exception due to no ET_r data being provided by DRI for the north east portion of that path. Overpass ET (mm/day) images were computed by multiplying the associated ET_rF images identified for use in the interpolation process by the ET_r for the date of the overpass. The ET_a images include values identifying areas outside the path AOI (as -99) and masked pixels (either buffered cloud mask or ET_rF values outside the range -0.05 to 1.5) as -9. Two Python scripts were used to conduct the time integration. The first script used linear interpolation to produce daily images of ET_rF and ET_a (produced as the product of daily ET_rF and daily ET_r). These daily images were sampled around ET flux tower sites to produce local ET_a maps for the sites. A second script summed daily ET_a and ET_r into monthly values and calculated monthly ET_rF by dividing monthly ET_a by monthly ET_r. The monthly ET_a, ET_rF and ET_r were combined into a three layer stacked image for each month and for the growing season (March – October).